

N O T I C E

THIS DOCUMENT HAS BEEN REPRODUCED FROM
MICROFICHE. ALTHOUGH IT IS RECOGNIZED THAT
CERTAIN PORTIONS ARE ILLEGIBLE, IT IS BEING RELEASED
IN THE INTEREST OF MAKING AVAILABLE AS MUCH
INFORMATION AS POSSIBLE

9950-328

ORL-69-DRD-SE-2
Technical Report: MRI-276

DOE/JPL-954977-79/9
Distribution Category UC-63

QUANTITATIVE ANALYSIS OF DEFECTS IN SILICON

Silicon Sheet Growth Development for the Large Area Silicon Sheet Task of the Low-Cost Solar Array Project

FINAL REPORT

by

R. Natash
J.M. Smith
T. Bruce
H. A. Qidwai

April 1980

JPL Contract No. 954977

MATERIALS RESEARCH, INC.
790 East 700 South Street
Centerville, Utah 84014
Phone: (801) 531-9600

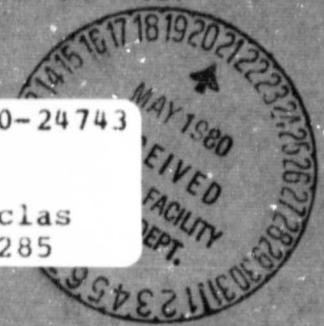
The JPL Low-Cost Silicon Solar Array Project is sponsored by the U.S. Department of Energy and forms part of the Solar Photovoltaic Conversion Program to initiate a major effort toward the development of low-cost solar arrays. This work was performed for the Jet Propulsion Laboratory, California Institute of Technology, by agreement between NASA and DOE.

(NASA-CR-163140) QUANTITATIVE ANALYSIS OF DEFECTS IN SILICON. SILICON SHEET GROWTH DEVELOPMENT FOR THE LARGE AREA SILICON SHEET TASK OF THE LOW-COST SOLAR ARRAY PROJECT Final Report (Materials Research, Inc.)

N80-24743

Unclas

G3/44 19285



DRL-69-DRD-SE-2

Technical Report: MKI-276

DOE/JPL-954977-79/9

Distribution Category UC-63

QUANTITATIVE ANALYSIS OF DEFECTS IN
SILICON

Silicon Sheet Growth Development for the Large
Area Silicon Sheet Task of the Low-Cost Solar Array Project

FINAL REPORT

by

R. Natesh
J.M. Smith
T. Bruce
H. A. Qidwai

April 1980

JPL Contract No. 954977

MATERIALS RESEARCH, INC.
790 East 700 South Street
Centerville, Utah 84014
Phone: (801) 531-9600

The JPL Low-Cost Silicon Solar Array Project is sponsored by the U.S. Department of Energy and forms part of the Solar Photovoltaic Conversion Program to initiate a major effort toward the development of low-cost solar arrays. This work was performed for the Jet Propulsion Laboratory, California Institute of Technology, by agreement between NASA and DOE.

TECHNICAL CONTENT STATEMENT

This report was prepared as an account of work sponsored by the United States Government. Neither the United States nor the United States Department of Energy, nor any of their employees, nor any of their contractors, subcontractors, or their employees, make any warranty, express or implied, or assumes any legal liability or responsibility for the accuracy, completeness, or usefulness of any information, apparatus, product, or process disclosed, or represents that its use would not infringe privately-owned rights.

C O N T E N T S

<u>SECTION</u>		<u>Page</u>
	LIST OF FIGURES	4
	LIST OF TABLES	7
I	SUMMARY	8
II	INTRODUCTION	10
III	TECHNICAL DISCUSSION	12
IV	RESULTS	28
V	CONCLUSIONS	34
VI	REFERENCES	35

LIST OF FIGURES

<u>Figure No.</u>	<u>Figure Title</u>	<u>Page</u>
1	IBM #1 - Section 1 - Area 1, micrograph of silicon ribbon surface showing intersection of three grains after cleaning organic materials from surface. 200X	36
2	IBM #1 - Section 1 - Area 2, micrograph of ribbon surface showing grain boundaries after cleaning organic materials from surface of ribbon. 200X	36
3	IBM #1 - Section 1 - Area 1, micrograph of ribbon surface after oxide removal. 200X	37
4	IBM #1 - Section 1 - Area 2, micrograph of ribbon surface, after oxide removal. 200X	37
5	IBM #1 - Section 1 - Area 1, micrograph of ribbon surface, after chemical polishing. 200X	38
6	IBM #1 - Section 1 - Area 2, micrograph of ribbon surface after chemical polishing. 200X	38
7	IBM #6 - Section 1 - Side 1, micrograph of ribbon surface after chemical polishing. 200X	39
8	IBM #6 - Section 1 - Side 1, micrograph of ribbon surface after a 15 second etch by Etching Solution I. 200X	39
9	IBM #6 - Section 1 - Side 1, micrograph of ribbon surface after a 15 second etch by Etching Solution I. 200X	40
10	IBM #6 - Section 1 - Side 1, micrograph of ribbon surface, after a 30 second etch by Etching Solution I. 200X	40
11	IBM #6 - Section 1 - Side 2, micrograph of ribbon surface after chemical polishing. 200X	41
12	IBM #6 - Section 1 - Side 2, micrograph of ribbon surface after a 30 second etch by Etching Solution II. 200X	41

LIST OF FIGURES (Continued)

<u>Figure No.</u>	<u>Figure Title</u>	<u>Page</u>
13	IBM #6 - Section 1 - Side 2, micrograph of ribbon surface after a 60 second etch by Etching Solution II. 200X	42
14	IBM #6 - Section 1 - Side 2, micrograph of ribbon surface after a 90 second etch by Etching Solution II. 200X	42
15	IBM #6 - Section 3 - Side 2 - Area 1, micrograph of ribbon surface after chemical polishing. 200X	43
16	IBM #6 - Section 3 - Side 2 micrograph of ribbon surface after a 60 second etch by Etching Solution III. 200X	43 & 44
17	Flow Chart of BASIC Program for QTM Operation and Data Reduction.	45
18 A,B,C	Photographs illustrating manual Image Editing in the "ACCEPT" mode on the QTM 720. 800X	46 & 47
19 A,B,C	Photographs illustrating manual Image Editing in the "PROJECT" mode on the QTM 720. 800X	47 & 48
20 A,B	Photographs illustrating manual Image Editing in "CUT" mode on the QTM 720. 800X	49
21	Graphical plot showing systematic variation in twin density with respect to specimen position in IBM Ribbon No. 4-457.	50
22	Histogram of grain boundary length of Mobil Tyco samples	51
23	Histogram of twin boundary density of Mobil Tyco samples.	52
24	Histogram of dislocation pit density of Mobil Tyco samples.	53
25	Histogram of grain boundary length of Motorola samples.	54

LIST OF FIGURES (Continued)

<u>Figure No.</u>	<u>Figure Title</u>	<u>Page</u>
26	Histogram of twin boundary density of Motorola samples.	55
27	Histogram of dislocation pit density of Motorola samples.	56
28	Diagram showing the position of Mobil Tyco samples MRI #19-30 as cut from ribbon 5-685.	57
29	Diagram showing the position of Mobil Tyco samples MRI #31-46 as cut from ribbons 5-742 and 5-744.	58
30	Diagram showing the position of Mobil Tyco samples MRI #47-77 as cut from ribbons 5-745, 5-743, 5-640 #1 and 5-640 #2.	59
31	Diagram showing the position of Mobil Tyco samples MRI #78-90 as cut from ribbon 5-867.	60
32	Diagram showing the position of Mobil Tyco samples MRI #91-98 as cut from ribbon 5-640.	61
33	Diagram showing the position of Mobil Tyco samples MRI #99-105 as cut from ribbon 5-990.	62
34	Diagram showing the position of Mobil Tyco samples MRI #106-134 as cut from ribbons 184-88, 184-175, 5-1094-33, and 5-1094-69.	63
35	Diagram showing the position of Motorola samples MRI #1-32 as cut from ribbons 6-792, 6-837, 6-656, and 6-840.	64
36	Diagram showing the position of IBM samples MRI #1-7 as cut from ribbon 4-457.	65

LIST OF TABLES

<u>Table No.</u>	<u>Title</u>	<u>Page</u>
1	Chemical polishing times of Wacker samples.	66
2	Chemical polishing times of IBM samples.	67
3	Chemical polishing times of Motorola samples.	68
4	Chemical polishing times of Mobil Tyco samples.	69
5-20	Data from QTM analysis of Mobil Tyco samples MRI #1-134.	70-85
21	Data from QTM analysis of IBM samples MRI #1-7.	86
22-25	Data from QTM analysis of Motorola samples MRI #1-32.	87-90
26	Listing of BASIC program "Defects in Silicon 3".	91
27	QTM data on Wacker sample.	94
28	QTM printout of data on Mobil Tyco sample MRI #100.	95

SECTION I
S U M M A R Y

The analyses of one hundred and seventy four (174) silicon sheet samples, about 1200 square centimeters, for twin boundary density, dislocation pit density, and grain boundary length has been accomplished. One hundred and thirty three (133) of these samples were manufactured by Mobil Tyco, thirty two (32) by Motorola, seven (7) by IBM, one (1) by Honeywell, and one (1) by Wacker.

Procedures have been developed for the quantitative analysis of the twin boundary and dislocation pit densities using a QTM-720 Quantitative Image Analyzing System. The QTM-720 system has been upgraded with the addition of a PDP 11/03 mini-computer with dual floppy disc drive, a Digital Equipment Writer (III) high speed printer, and a Field-Image Feature Interface Module (F.I.F.I.). These changes have greatly enhanced the speed and reliability of the QTM-720 System as well as improving the data storage and printout capability.

Three versions of a computer program that controls the data acquisition and analysis on the QTM-720 have been written.

Procedures for the chemical polishing and etching of Mobil Tyco, Motorola, IBM, & Wacker samples have been developed.

This report describes the complete procedures for the defect analysis of silicon samples using a QTM-720 Image Analyzing System, and includes chemical polishing, etching, and QTM operation. The data from one hundred and seventyfour (174) samples, and a discussion of the data is also included herein.

In addition to the above work, comparisons of the capabilities of a variety of powerful analytical techniques in analyzing impurities from four different silicon matrix was performed. The silicon matrix analyzed were Mobil Tyco (EFG-RH and EFG-RF), Honeywell (SOC), and Motorola (RTR). The techniques used were: Neutron Activation Analysis, Spark Source Mass spectrometry, Ion Scanning Spectrometry, Secondary Ion Mass Spectrometry, Scanning Auger Microanalysis, Electron Spectroscopy for Chemical Analysis, Ion Microprobe Mass Spectroscopy,

and Optical Microscopy. The results showed significant differences in the capability of the various analytical techniques for analyzing silicon impurities and, in addition, provided important information regarding the type and distribution of impurities present in the various silicon matrix. The details of this work is presented in a separate report (MRI-267) to JPL.

SECTION II

INTRODUCTION

The main objective of this program was to develop imaging techniques to subsequently allow rapid, reproducible, and accurate evaluation of silicon sheet defect structure. Secondly, defect data accumulated for many samples would allow for potential cross correlation between structures revealed and specific sheet fabrication technique and/or efficiency. Structural defects that were quantified included grain and twin boundaries, precipitates, and dislocations. Quantitative characterization of these structural defects, which have been revealed by etching the surface of silicon samples, can then be performed using a Quantimet 720 Image Analyzer.

The silicon sheet samples were originally obtained by JPL from different manufacturers. Each of these manufacturers use their own crystal growth and fabrication techniques and, therefore, the various types of silicon produced contain a variety of trace impurity elements and structural defects. The most important criteria in evaluating the various silicon types for terrestrial solar cell applications are: (i) cost, and (ii) conversion efficiency. At present, the solar cells with highest conversion efficiency are made of high purity silicon single crystals, which are free from structural defects such as dislocations, twin boundaries, precipitate particles, etc. But these crystals and subsequent processing are very expensive and may not meet the DOE goal of 50 cent/watt by 1986. On the other hand, silicon crystals such as Edge-defined Film-fed Growth (EFG) ribbons, Silicon on Ceramic (SOC), Wacker, etc, are NOT single crystals; but made of highly ordered crystals which contain large and differing numbers of dislocations, twin boundaries, grain boundaries, and precipitates compared to the premium grade or Czochralski grown silicon.

The following important questions must be answered to evaluate low and high cost silicon sheet: (i) What effect do these defects have on conversion efficiency? (ii) Of the various types of defects, which defect/defects severely affects conversion efficiency? (iii) At what concentrations does this effect become significant? (iv) Is there a rapid, accurate, quantitative method that can be used routinely as a Quality Assurance tool?

Quantitative analysis of surface defects was developed and is being performed by using a Quantimet 720 Quantitative Image Analyzer. This system can differentiate and count 67 shades of grey levels between black and white contrasts. In addition, it can characterize structural defects by measuring their length, perimeter, area, density, spatial distribution, frequency distribution (in any preselected direction), and is programmable in these measurements. However, the Quantitative Image Analyzer is extremely sensitive to optical contrasts of various defects. Therefore, to obtain reproducible results, the contrasts produced by various defects must be similar and uniform for each defect types along the entire surface area of samples to be analyzed. To achieve this, a chemical cleaning and polishing technique has now been perfected for silicon samples from Mobil Tyco, Wacker, Motorola, and IBM. The cleaning and polishing preparation technique produces a very clean and even surface for silicon crystals suitable for analyses by the QTM 720 Image Analyzer. We have now obtained quantitative information from a variety of silicon crystals.

SECTION III

TECHNICAL DISCUSSION

As mentioned in the introduction, it has been found necessary to chemically polish silicon samples before analyzing them with QTM. The chemical polishing procedures are discussed below:

CHEMICAL POLISHING

The first step in the chemical polishing process is to clean the surfaces of the silicon crystals. This is achieved by rubbing the surfaces with swabs soaked in trichloroethylene. This process removes most of the organics from silicon surfaces. However, to remove remaining residues and water spots, an acetone rinse followed by ethyl alcohol rinse are required. Silicon surfaces are then dried by blowing nitrogen or freon gas over them. Figures 1 and 2 show the silicon surfaces after cleaning. All optical micrographs were taken in a Baush & Lomb metallograph.

An acid resistant protective coating is applied to one surface of the silicon sheet sample in order to prevent it from being polished. This allows MRI to complete the etching and defect analyses & then send the silicon samples back to JPL. JPL may then remove the protective coating from the unpolished surface, and process the sample into a solar cell and measure its conversion efficiency. This will allow JPL to determine the effects, if any, of the density and type of structural defects to conversion efficiency. Since both these data are obtained on the same silicon sample, the results obtained will be of significant value in determining the effects, if any, of structural defects on the performance of solar cells.

Of the various coating materials studied, Apiezon Wax (W) gave best results. This is resistant to many acids at 80°C for at least 120 seconds. A solution is prepared by dissolving a very small amount of Apiezon Wax (W) in trichloroethylene. This solution is sprayed by air brush or applied by a fine paint brush to one of

the silicon crystal surfaces. The surface is then baked for 10 ± 1.0 minutes at $125^{\circ}\text{C} \pm 10^{\circ}\text{C}$. Baking is necessary to evaporate the trichloroethylene and allow the wax to flow uniformly on the surface.

In order to start with a uniform surface for acid polishing, any SiO_2 coating on the silicon sample surface must be removed. This is done by immersing the sample in concentrated HF for 2 minutes at room temperature. The sample is rinsed in deionized water, and ethyl alcohol respectively. Freon gas is used to dry the sample surface. Figures 2 and 4 show the silicon surfaces after removal of the SiO_2 layer. Only a few angstroms thick layer of SiO_2 is covering the surface of silicon samples, therefore, the removal of this SiO_2 layer does not significantly alter the microstructure as may be seen by comparing Figs. 1 and 3; and Figs. 2 and 4.

The most suitable polishing solution for silicon surfaces is a mixture of 70% HNO_3 : 49%HF:99.9% CH_3COOH in 1:2:3 ratio by volume. All acids used were Electronic Grade, Low Sodium MOS quality. The polishing solution is heated to $50^{\circ}\text{C} \pm 3^{\circ}\text{C}$ in a teflon beaker on a hot plate. The silicon sample is then immersed in this solution. It has been found that silicon samples from different manufacturers require varying polishing times. The polishing times required for Mobil Tyco, Motorola, IBM, and Wacker samples are summarized in Tables 1 to 4.

The polished samples is then rinsed in deionized distilled water for 5 minutes, followed by rinsing in ethyl alcohol. It is then dried by blowing freon gas on the surface.

It may be noted that samples which are slightly underpolished as well as samples which are well-polished, exhibit bright and shiny surfaces when observed by the naked eye. Therefore, visual observation can not be used to determine the quality of polishing. However, when the samples are observed at high magnifications (800 X or greater) in a high quality optical metallograph, the underpolished samples show growth lines and overpolished samples show faceting and sub-grain type structure, whereas the well-polished samples show clearly

defined grain boundaries and some of the twin boundaries in sharp contrast. Therefore, an optical metallograph must be used to determine the quality of polishing.

Figures 5 and 6 show the polished surfaces of silicon samples.

After the silicon samples are chemically polished, they are etched to reveal structural defects.

CHEMICAL ETCHING:

The etching solution that has been developed is a dilute variation of the Sirtl etch. Composition of the Sirtl etch is as follows:

<u>Solution A</u>	<u>Solution B</u>
50g CrO ₃ :100 ml deionized water	49% HF, electronic grade Solution B equal in volume to Solution A

Three dilute variations were prepared from the Sirtl etch. The results obtained by using each of these three etchants are discussed below:

ETCHING SOLUTION I:

The first variation from the Sirtl etch was prepared by dissolving 20 grams of CrO₃ in 60 ml of deionized distilled water, and then adding an equal volume of concentrated HF. A 15 second etch by this first etching solution revealed dislocations, twin boundaries, and grain boundaries. The resolution of the defects are limited only by the optical equipment used.

Figure 7 shows the structure of an IBM silicon ribbon after chemical polishing. Figures 8 and 9 are photomicrographs after a 15 second etch.

The variation in contrast between different boundaries may be indicative of different energies associated with different types of boundaries. Grain boundaries and twin boundaries have different energies, which may affect their etching rates.

An additional 15 seconds etch by the Etching Solution 1 revealed a higher number of defects and less contrast variation between different twin boundaries (Figure 10).

ETCHING SOLUTION II

The second variation from the Sirtl etch was prepared by dissolving 10 grams of CrO_3 in 40 ml of deionized water, and adding an equal volume of concentrated HF.

Figure 11 is a photomicrograph of the chemically polished surface. Figure 12 is a photomicrograph of the same surface after 30 seconds etch by Etching Solution II. Figure 12 shows all dislocations, twin boundaries, and grain boundaries present in the sample. Variations in contrast of dislocations is, however, due to focusing on a slightly curved surface.

The silicon surface in Figure 12 was etched for an additional 30 seconds. This resulted in deeper etching of dislocations and overlapping of twin boundaries (Figure 13). An additional 30 seconds etch (i.e., a total of 90 seconds) on the same surface resulted in significant overlapping of dislocations and twin boundaries (Figure 14).

ETCHING SOLUTION III

The third variation from the Sirtl etch comprises 10 grams of CrO_3 in 60 ml of deionized distilled water; and an equal volume of concentrated HF.

Figure 15 is a photomicrograph of a chemically polished silicon surface. Figure 16 is a photomicrograph of the same area after 60 seconds etch by Etching Solution III.

The etching treatment by Etching Solution III resulted in an optical resolution of 10^{-4} cm for twin boundaries and an optical density resolution of 10^7 dislocations per cm^2 at magnifications of 800X and above. A higher resolution, however, can be achieved if a higher magnification is used for observation.

It has been observed on many silicon surfaces that an optimum etching time of approximately 50 seconds by Etching Solution III is sufficient to distinctly reveal grain boundaries, twin boundaries, and dislocations. Etching Solution III has been used to etch Mobil Tyco, Motorola, IBM, Wacker, and Honeywell samples.

High quality defect structures without overlapping and without wide variations in contrast of each defect type were always obtained.

USE OF THE QTM 720-PDP 11/03 SYSTEM FOR IMAGE ANALYSIS:

During the months of March and April, 1979, changes were made to the QTM system to allow for more efficient data storage and analysis capabilities.

Before these changes, the QTM 720 was run in a semi-automated fashion¹, making use of a Hewlett-Packard Model 9810 programmable calculator interfaced to the system by means of a special QTM module, the Field Data Interface. In addition, the data output was printed on a conventional teletype. In the present configuration, a PDP 11/03 with a Digital Equipment Corporation Writer (III) and a RX01 dual floppy disc drive is interfaced to the QTM-720. Two special QTM modules are used for the interfacing: a Field-Image-Feature Interface (FIFI) and a Control Interface (CI).

The FIFI links the QTM 720 to the PDP 11/03 computer allowing high speed data transfer from the QTM directly into the memory of the PDP 11/03. The Control Interface permits QTM module switching instructions to be transferred from the PDP 11/03 directly to the QTM. Both FIFI and CI are under the control of BASIC language, and programs may be written on the PDP 11/03 to perform module switching, as well as data acquisition and analysis.

The following section gives specific instructions for the system operator so that, given a silicon wafer which has been properly polished and etched, the wafer is viewed with the microscope interfaced to the QTM 720 Image Analyzer. The following section gives detailed instructions to the operator for the actual sample run.

The following QTM 720 modules are used in the present system configuration: ID Auto Detector, MS-3 Standard Computer, two Function Computers, Classifier/Collector, Variable Frame, Control Interface, Image Editor, Auto Focus, X-Y Stage Control, and the Field-Image-Feature Interface.

PREPARATION FOR SAMPLE RUN

1. Select proper objective on the microscope for desired magnification (a total optical magnification of X800 is normally used).
2. Adjust optics for "Kohler illumination," following steps in the microscope manual², if necessary. It is important that the field of view be uniformly illuminated so that features of interest will be detected uniformly.
3. Adjust the light intensity (with filters and/or lamp voltage) to obtain a reading of 1 on the white level meter with light sensitivity switch in MANUAL. The sensitivity is then set to AUTO.
4. Place the sample on a blank field of view and perform shade correction, setting the RANGE at about 10-11 o'clock. If a suitable blank field cannot be found, one may de-focus the field of view so that no distinct features may be identified, and a relatively uniform, featureless field is observed. For best results, the entire standard frame should be detected as uniformly as possible. (Light sensitivity switch should be in AUTO to perform shade correction.)
5. Place sample at the origin of the scan, which will be the lowest left-hand corner of the sample. Make certain that the sample is firmly held to the stage. Select the size of the X-Y step on the automatic stage control. Generally, the X and Y steps will be of the same size (units are in mm). Determine the number of steps in a single row (X-direction). (The number of fields in a row is one greater than the number of X steps). After setting the number of steps on the automatic stage control, place control in AUTO and push ORIGIN. Whenever manual control of the stage is desired, switch from

- AUTO to MANUAL. When returning to AUTO mode, stage must be at ORIGIN. Always set ORIGIN after pushing AUTO. At this time, set the Automatic Focusing module to AUTO and SKIP FIELDS to zero.
6. Determine the size of the Variable Frame to be used for scanning and position it. The product of the horizontal and vertical divisions (in picture points) will be the frame area called for at the beginning of the program.
 7. There are two twisted-pair leads in the back of the FIFI module which feed into BIG FRAME OUT and VARIABLE FRAME OUT. It is necessary to interchange these leads if it is desired to perform measurements on dislocations and twin boundaries. For the analysis of twin boundaries, the full frame (500,000 picture points) of the T.V. screen is used. This is because the twin boundaries remain in focus over the entire screen area. But for the dislocation pits, half the frame (250,000 pp) is used. This is because the dislocations tend to go out of focus near the edges of the full frame. It will be necessary to determine manually the average feature area (in pp) by sampling several fields throughout the sample. This value is called for in the program. (Note: The automatic stage will have to be placed in the MANUAL mode during this operation, followed by step 5 above).
 8. Set proper detection of the features in the field using the "flicker method" and the Detector Module.
 9. The Standard Computer, both Function Computers, and the Classifier-Collector should be set to AUTO.

PREPARING THE PDP 11/03 FOR OPERATION OF THE QTM-720

1. Place the System floppy disc into the left-hand drive of the RX01 dual disc drive and the data file storage disc into the right hand drive. Turn on power to the PDP 11/03 and to the DECWRITER. "Boot" the system

in the sequence ENABLE-DC-LTC. The symbol \$ will appear on the
DECWRITER

2. Type DX <CR> and the message "RT-11SJ V02C-02H" will be returned.
3. Type the current date in the format DATE 06-Jun-79 <CR>.
4. Type R QBS203 <CR>, and the symbol * will be returned. Input a carriage return, <CR>, and the message "READY" will be typed out.
5. The current program for defect characterization of silicon is program DS2. Therefore, type OLD "DS2" <CR> and upon obtaining the "READY" response, again type RUN <CR>.
6. The following steps describe where necessary the information called for as input data for the program:

HEADING - Any one line description of the current run.

PRINT FILE NAME . . . - This is the name of data file on the
appropriate floppy disc where this run will be stored.

OPERATOR - Name of operator.

MAGNIFICATION

UNITS

CALIBRATION FACTOR (UNITS/PP)

FRAME AREA (PP) - The Standard Frame area is 500,000 pp.

QTM OUTPUT DATA DIVIDED BY - It may be necessary to use the
classifier-collector module to divide the QTM output data
by a power of ten if the OVERFLOW light comes on during
sample analysis.

AVERAGE FEATURE AREA (PP) - This must be determined manually before
the sample run.

7. The heading for the data output is now printed. The raw data in units of picture points will be typed out in parentheses for each field. These are the actual QTM measurements of the detected features within the frame area in the order : area, perimeter, vertical projection, and horizontal projection.

After the parameters are printed out for each field, a question mark is printed. If a carriage return, <CR>, is typed, the next field will be measured and printed out. However, if a D is typed, then the data acquired in the last field of measurement is deleted and the message "LAST FIELD DELETED" is printed.

If an A is typed in response to the question mark, the average of each parameter, along with its standard deviation and standard error of the mean, is printed. The average is taken for all measurements previous to this time, except for fields deleted. Following the average, the field numbers continue consecutively. The average values for Mean Free Path are determined by dividing the cumulative sum of the frame areas by the cumulative sum of the projection. In this case, standard deviation and standard error are not defined.

COMPUTER PROGRAMMING FOR THE PDP 11/03

The PDP 11/03 minicomputer controls many of the functions of the QTM-720 Image Analyzing System. Programming for this minicomputer determines how the raw data from the QTM is analyzed. Three versions of a computer program designed to analyze the data from silicon samples have been written. The current program being used is "Defects in Silicon 3", which analyses the raw data faster and allows for a more convenient printout format than in the previous two versions. A Flow Chart of this program is shown (Fig. 17) along with a listing of the BASIC program "Defects in Silicon 3" (Table 26).

MANUAL INTERACTION WITH THE QTM 720

In many situations when analyzing silicon samples with the Quantimet 720, it is necessary to manually edit the image that is being detected. These include situations where extraneous features are present on the surface of the sample such as dust particles or stain marks. Also, due to the unevenness of the sample surface in some locations the entire area in a field cannot be focussed, causing detection problems in the unfocussed areas. In many cases clusters of dislocation pits are joined to the twin boundaries causing the QTM to detect a larger twin area than is really present. In such cases, manual image editing can be used to overcome these problems.

Image editing on the QTM 720 is performed by the use of a light pen coupled with the Image Editing Module. The light pen is used to indicate on the QTM screen the areas or features that are to be edited or manually manipulated. The Image Editor is capable of specifying particular regions or features for measurement and rejecting others. The Image Editor is also capable of filling in imperfectly detected features or separating features that are touching.

The use of the Image Editor as it pertains to the analysis of silicon samples is illustrated by the photographs shown in Figures 18A through 20B.

The first three photographs, Figures 18A through 18C, show the operation of the image editor in the ACCEPT mode. The photograph in Figure 18A shows the QTM screen with the image of a polished and etched silicon sample* displayed. A large field of dislocations can be seen on the left side of the picture with a heavy band of twins running down the center. On the right side of the screen, clusters of dislocation pits are present. The top of the QTM display screen indicates that the image editor is in the "ON" position, and in the ACCEPT mode, and also indicates the count in picture points of the features detected.

*Mobil Tyco # 53, JPL 145-7E, 5-745, SPEC. G.

In Figure 18A, the number 13 refers to the counts from the previous field and should be ignored. In Figure 18A, the light pen is shown being used to circle a region that is to be accepted for detection. When the DETECT switch is pushed on the QTM, the area that has been accepted is displayed on the screen while all other areas are not displayed. This is shown in Figure 18B. Only the features in this region will be counted by the QTM and all other features will be ignored. The photograph shown in Figure 18C shows the same specimen area with only the dislocation pits being accepted, and all the twins rejected.

The REJECT mode of the Image Editor operates in much the same way as the ACCEPT mode. This operation is illustrated in the photographs shown in Figures 19A through 19C. In Figures 19A, 19B, and 19C the same specimen area is shown as in the previous photographs.

On the right side of the photograph in Figure 19A, the operator's hand can be seen with the light pen circling an area to be rejected. In Figure 19B, the light pen is pointing towards the region that has been rejected. The features in this region are no longer displayed on the screen when the DETECT switch is pushed on, and these features are no longer counted. Figure 19C shows the same specimen area with most of the dislocation pits rejected leaving only the twins displayed. In these three Figures 19A, 19B and 19C, the count of features detected in picture points is indicated as 87, 79 and 13 respectively. The detected feature count was being divided by 100 when these samples were analyzed. The actual number of counts in picture points are 8700, 7900, and 1300. The 1300 counts in Figure 19C are from the residual dislocation pits that have not been rejected. In order to determine the number of dislocations being counted, these numbers must be divided by the average feature area for dislocations, which range between 5 and 10 picture points depending on the sample.

The Image Editor can also be used to separate features which are touching one another. To do this, the Image Editor is put into the CUT mode. This is illustrated in the photographs in Figures 20A and 20B. Figure 20A shows a region containing dislocation pits with a single twin boundary running down the center. Some of the dislocations are touching the twin boundary and, therefore, are being included in the total twin area count. The twin area is indicated as 3183 picture points. In Figure 20B the light pen has been traced around the twin with the Image Editor in the CUT mode. This separates the twin from the adjoining dislocation pits. The feature area count is the 2870 picture points, which is the true area of this twin.

The Image Editor need not be used in the analysis of silicon samples if the sample surface is flat and well-polished. However, in samples that are uneven, or in samples where large fields of dislocations are connected with twins, image editing must be used to obtain accurate results.

MEASUREMENT OF TWINS AND DISLOCATION PITS:

In all of the samples analyzed, except the Wacker samples, most of the twins are oriented parallel to one another and run from one edge of the wafer to the opposite edge (parallel to the longitudinal axis of the silicon ribbon, the growth direction). Therefore, in order to measure twin density, 50 fields were chosen along the central transverse axis of the sample perpendicular to the growth direction. In other words, the central transverse axis is perpendicular to the twins. The distance between each of these 50 fields where measurements for twins were made was 0.31 mm. The long dimension of each field was 0.30 mm. Thus, each of these fields were adjacent to one another by a distance of 0.01 mm and, therefore, did not overlap one another. It is important that the fields do not overlap, since the same twin should not be counted twice. At the same time, the fields must be close to one another so that almost all the

twins are counted by the QTM. On the other hand, counting may also be done using a square raster of 50 fields distributed evenly over the entire sample surface. In this case, the horizontal distance separating each field will be 2.5 mm, which is much larger than the long dimension of the frame i.e., 0.30 mm. Therefore, under the method of square raster, there is a possibility that areas in the sample where the twin or dislocation density is very high may not be counted. This will result in large errors. Therefore, all the 50 fields were counted along the central transverse axis of the samples.

It has also been found that the density of dislocation pits in the samples have longitudinal symmetry similar to the twins. Therefore, for dislocation pit density measurements, all the fifty fields were chosen along the central transverse axis of the silicon samples.

MEASUREMENT OF AVERAGE AREA OF TWINS AND DISLOCATION PITS:

Before measurements were made for twins, each sample was scanned to determine manually the average area of one twin. The method of determining the average twin area is as follows: First, the sample surface was randomly scanned, and those fields were selected where the twins were not touching each other. Each field, generally containing more than 5 distinct twins, were then displayed on the display module of the QTM. The total area of all the twins in each field was determined and divided by the number of twins in that field to get the average twin area for that field. The average twin area was then determined in an additional 4 fields. The arithmetic average was then calculated from the average twin area in these five fields. Generally, 30 to 40 twins were used in 5 fields to get the average twin area. The same procedure was used to obtain the average dislocation pit area. The average twin area in each sample was then fed into the QTM software. This is an important step to get the actual number of twins and dislocation pits, especially in areas where

the densities of these defects are high and they touch one another. In order to verify that the average area of a twin so obtained was accurate, an additional six fields were selected at random where the twin density was high, and the twins were touching one another. The twin density in each of these six fields were counted manually, and also counted by the QTM using the average area of a twin. The entire procedure was repeated until close agreement was reached between manual counting and QTM counting. After this procedure, measurements were then made on all the fields using the automatic QTM mode.

EXPLANATION OF COMPUTER PRINTOUTS:

In the computer printouts, the first paragraph shows the name of the computer program and date.

The second paragraph shows the MRI and JPL sample numbers.

The third paragraph lists; 1) the name/names of the operator; 2) magnification being used (800X); 3) units used i.e., mm for twins, and microns for dislocation pits; 4) calibrated equivalent value of one picture point in the units being used; 5) frame area used; 6) QTM output data was divided by 100 and corrected in the case of twin measurements to avoid frequent overflow problems in the Classifier-Collector. In the case of dislocation pits, the data was divided by 1 as indicated in the computer printouts; 7) average feature area (pp), for twins and dislocation pits.

All the information listed in the third paragraph of the computer printouts were fed into the computer on its command before collecting the data using the automatic mode.

The frame area of a standard frame in the QTM is 500,000 picture points (pp). In case of twins, the standard frame was used. However, during dislocation density measurements the uneven sample surfaces caused problems in focusing dislocation pits over the entire standard frame. Therefore, during dislocation density measurements half the standard frame (250,000 pp) was used. This is listed

as "Frame Area" in the QTM data sheets. The unit of measurement was millimeter for twins, and microns for dislocation pits.

The fourth paragraph of the computer printout lists the titles for the different measurements, which are explained below:

FLD: (A, P, VP, HP) indicates the sequence number of the field in which measurements were made. The raw data in terms of picture points are also shown in parentheses. The raw data listed is area, perimeter, vertical projection, and horizontal projection of the detected features in each field.

NO. denotes the total number of features detected in any field. This is obtained by dividing the total area of a feature by the average area of that feature.

No./AREA: denotes the computed number of features/mm² or features/microns² in each field.

MFPV: denotes the mean free path in the vertical direction. This quantity is the frame area divided by the vertical projection of all detected features in the field (frame).

MFPH: denotes mean free path in the horizontal direction. This is the horizontal analogue of MFPV.

L/A: This quantity is length of detected features per unit area. The unit area is mm² in the case of twins, and microns² in the case of dislocation pits.

The quantity L/A is subject to large errors when twin bands are present. The QTM computes L/A by dividing the perimeter by 2. A twin band usually contains 20 to 100 individual twins, many of them touching one another. The QTM will compute L/A by dividing the perimeter of the twin band by 2. In other words, the QTM may count the entire twin band as one large area rather than consisting of several individual twins. Thus, L/A is subject to large errors and is underestimated by QTM.

The attached computer printouts show, after 25 and 50 fields, the computed values of average, standard deviation, and standard error for all data from field No. 1 onwards. This averaging can be done at any time during the course of the measurement (Table 28).

The grain boundaries in each sample were counted under the binocular microscope using 7X magnification. Most of the grain boundaries were parallel or approximately parallel to the twins.

Due to the large volume of computer printouts, all of these printouts will not be included in this report but are available in Quarterly Progress Reports (MRI-255, MRI-260, MRI-264, MRI-269, MRI-273). The data on twin boundary density, dislocation pit density, and grain boundary length have been summarized in Tables 5 to 25.

A complete computer printout for Mobil Tyco sample MRI #100 is shown in Table 28 to illustrate the data printout format. The data for all of the Motorola samples, Mobil Tyco samples MRI 78-134, and Honeywell sample are recorded on floppy discs. The data from the other samples are recorded on paper tape.

SECTION IV
R E S U L T S

A total of one hundred and seventyfour (174) silicon samples, approximately 1200 square centimeter, have been analyzed to date. One hundred and thirtythree (133) of these samples were manufactured by Mobil Tyco, thirtytwo (32) by Motorola, seven (7) by IBM, one (1) by Honeywell, and one (1) by Wacker. These samples were analyzed for twin boundaries, grain boundaries, and dislocation pits. Twin boundary and dislocation pit measurements were made using the QTM-720 as described in this report, and grain boundary measurements were made using a binocular microscope at 7X magnification. Data from these measurements are summarized in Tables 5 to 25. Histograms showing the distribution of twin boundary density, dislocation density, and grain boundary length in the Mobil Tyco and Motorola samples are shown in Figures 22 to 27.

Due to the large number of computer printouts containing the data on the 174 samples analyzed, these printouts are not included in this report. The information is available on floppy discs for later analysis, however. The data on vertical mean free path (VMFP) and horizontal mean free path (HMFP) have not been summarized and included in this report. It is unclear at present whether this data will be pertinent to the correlation of defect density with conversion efficiency. If it is found to be useful, this data will be included in later reports.

Diagrams showing the sample position as cut from the ribbons for the Motorola samples, the IBM samples, and Mobil Tyco samples 19-134 are shown in Figures 28 to 36. Also, on these diagrams are listed the dislocation pit and twin densities as found by QTM analysis.

MOBIL TYCO SAMPLES

Two types of Mobil Tyco EFG Silicon samples have been analyzed. Mobil Tyco EFG -RH (Resistance Heating) and Mobil Tyco EFG -RF (Radio Frequency Heating) samples.

Mobil Tyco samples MRI #1-18 are EFG -RH samples. These samples have fairly low dislocation and twin boundary densities as compared with later analyzed Mobil Tyco samples. The average dislocation density for these samples is 0.0107 dislocations/ μm^2 and the average twin boundary density is 308.7 twins/ mm^2 (as calculated from Table 5).

Mobil Tyco samples MRI #19-30 are EFG-RH samples. These were some of the first Mobil Tyco EFG-RH samples to be manufactured and contain a large number of SiC particles. The number of SiC particles in these samples are listed in Table 6. These samples contain very large dislocation densities. The average dislocation density for these samples is 0.0748 dislocations/ μm^2 . The average twin density for these samples is 261.79 twins/ mm^2 , and the average grain boundary length/ cm^2 is 1.14 . The high dislocation density of sample MRI #19-30 seems to indicate that dislocations tend to nucleate around SiC particles. This high dislocation density around precipitate particles has also been observed by other researchers in EFG ribbons³. The highest local dislocation density found in samples 19-30 was $.407$ dislocations/ μm^2 which corresponds to a density of 4.07×10^7 dislocations/ cm^2 . This local dislocation density was found in sample MRI # 30. The average dislocation density in this sample is $.084$ dislocations/ μm^2 or 8.4×10^6 dislocations/ cm^2 . These samples have slightly lower grain boundary length/ cm^2 than the other Mobil Tyco samples.

In the later Mobil Tyco samples, few SiC particles were found and lower dislocation densities were observed.

Mobil Tyco samples 31-77 are of the type EFG-RF. The twin boundary density, dislocation pit density, and grain boundary length are listed in

tables 7 to 12. The average dislocation pit density for samples 31-72 is $.0408$ dislocations/ μm^2 , the average twin density was found to be 556.93 twins/ mm^2 , and the average grain boundary length/ cm^2 is 1.86 .

Mobil Tyco samples 78-134 are of the EFG -RH type. The average dislocation density for these samples is $.0292$ dislocations/ μm^2 , the average twin density is 750.49 twins/ mm^2 , and the average grain boundary length/ cm^2 is 2.95 . The mean defect densities for all the 133 Mobil Tyco are 0.037 dislocations/ μm^2 (Fig. 24), 540.4 twins/ mm^2 (Fig. 23), and 2.35 cm/cm^2 grain boundary length.

As mentioned previously most of the twins in the Mobil Tyco samples run longitudinally through the ribbons, therefore samples cut from the same ribbon, or from the same side of a ribbon tend to have similar twin densities. Detailed discussions of the twinning process for EFG ribbons are presented in references 4 and 5. Dislocation pit density also has some longitudinal symmetry, but the dislocation pit density is more variable from sample to sample in the same ribbon. The highest dislocation density in the Mobil Tyco samples is found in areas where few twins are present, and in heavy twin bands few dislocations pits are found. The highest local dislocation pit density was found in sample MRI No. 101 and is $.528$ dislocations/ μm^2 , i.e., $5.28 \times 10^7/\text{cm}^2$.

The surfaces of all of the Mobil Tyco samples are very uneven with surface ripples. These surface ripples have been observed by other researchers and are described in more detail by De Angelis⁶.

Figures 28 to 34 are diagrams showing the position of the Mobil Tyco samples as cut from the ribbons. The twin density and the dislocation pit density are shown on these diagrams.

MOTOROLA SAMPLES:

Data on twin boundary density, dislocation pit density, and grain boundary length for thirty two Motorola samples are summarized in Tables 22 to 25.

Figure 35 indicates the sample position as cut from the Motorola ribbons. The figure also indicates the twin boundary and dislocation pit densities. Figures 25, 26, and 27 are histograms relating twin boundary densities, dislocation pit densities, and grain boundary length to the number of samples analyzed.

There is no clear cut relationship between twins, grain boundaries, and dislocation pits among these samples whether cut from the same ribbon or when samples from different ribbons are compared.

Specimens from the ribbon 6-840 contains the lowest twin and dislocation densities (especially, sample 6-840 G). This ribbon, however, has very high grain boundary length/cm². In general, the twin, dislocation pit, and grain boundary measurements for the other specimens taken from the ribbons 6-792, 6-837, 6-656, and 6-791 are comparable in magnitude.

There are large variations in the twin boundary, dislocation pit, and grain boundary measurements for individual samples from the same ribbon. For example, for the ribbon 6-840 the highest twin density is 1272.02 twins/mm² and lowest twin density is 157.91 twins/mm². The highest dislocation density from this ribbon is .0129 dislocations/μm² and the lowest is .0014 dislocations/μm².

There seems to be no relationship between twin boundaries, dislocation pits, and grain boundaries with respect to the specimen position on the ribbon.

The average dislocation pit density for all of the Motorola samples is .0136 dislocation pits/μm², the average twin density is 1032.21 twins/mm², and the average grain boundary length/cm² is 3.27 (Figs. 25, 26, and 27).

As compared with the Mobil Tyco samples, the Motorola samples have a higher average grain boundary length and a higher twin density, but have a lower average dislocation density. It can be seen however, that the Motorola samples have a larger variation in twin density, dislocation pit density, and grain boundary length than in the Mobil Tyco samples. In the Motorola samples, the twin boundaries

and dislocation pits have the same longitudinal symmetry as in the Mobil Tyco samples, but the twin bands and dislocation pit areas seem to be more intermittent, and do not run throughout the whole length of the ribbons. This explains why samples cut from the same ribbon have such a large variation in defect densities.

IBM SAMPLES

Data on twin boundary density, dislocation pit density, and grain boundary length for seven (7) IBM samples are listed in Table 21. The average dislocation density for the IBM samples is .010 dislocation pits/ μm^2 , the average twin density is 499.64 twins/ mm^2 , and the average grain boundary length/ cm^2 is 1.11.

The IBM samples were the only samples analyzed that seemed to have a systematic variation of defect density with respect to specimen position as cut from the ribbon. This variation is shown graphically in Figure 21. This figure indicates that twin boundary density decreased as the ribbon was grown. No such variation was found in these samples for dislocation pit density or for grain boundary length.

HONEYWELL SAMPLE

The Honeywell sample consisted of a ceramic substrate coated with a film of silicon. The densities of dislocations, grain boundaries, and twin boundaries are listed in Table 1. The dislocations tended to be more evenly distributed throughout the Honeywell sample than in the Mobil Tyco samples and the dislocation density is slightly less. The twin density in this sample is also lower than that found in the Mobil Tyco samples.

The twin boundaries and dislocation pits tended to have longitudinal symmetry as in the Mobil Tyco and Motorola samples.

The surface of the Honeywell sample shows ripples that are approximately 2 mm apart and run perpendicular to the twin boundaries.

WACKER SAMPLE:

One Wacker sample was analyzed for twin boundaries on the QTM; the printout of data on this sample is listed in Table 27. Unlike the other samples analyzed, the twin boundaries in the Wacker samples do not run parallel to one another. The twins within different grains are oriented in different directions. To further complicate the counting of these defects, all of the twin boundaries intersect the grain boundaries, and there are a large number of such intersections in each field of view.

Wacker sample No.7 was the first sample to be analyzed on the QTM. This sample had a surface area of 40.32 mm². As shown in Table 17, a total of 50 fields (or frames) were analyzed on the QTM. These 50 fields were uniformly distributed in a square raster covering the entire sample surface.

The average twin density was found to be 15.8 twins/mm², which is much lower than that found in the other samples analyzed. The grain boundary length in these samples, however, is much higher than in the samples from other manufacturers, although grain boundary length/cm² was not quantitatively determined for the Wacker sample.

SECTION V

CONCLUSIONS

Procedures have been developed for the analysis of defects in silicon sheet using a QTM-720 Image Analysis system. The analysis technique proved to be rapid, accurate, and reproducible.

Chemical polishing and etching techniques have been developed that can effectively reveal structural defects and prepare the silicon surface for automatic QTM analysis. These procedures have been developed for Mobil Tyco, Motorola, IBM, Honeywell, and Wacker samples.

One hundred and seventy four (174) silicon samples, approximately 1200 square centimeter surface area, have been analyzed for twin boundary density, dislocation pit density, and grain boundary length. The data from these samples being included herein.

The samples analyzed under this contract have been returned to JPL and may be manufactured into solar cells with the electrical conversion efficiency measured. The conversion efficiency can then be correlated to the defect density and quantitative relationships obtained between twin boundary density, dislocation density, grain boundary length, and conversion efficiency.

SECTION VI

R E F E R E N C E S

1. R. Natesh, J. M. Smith, H. A. Qidwai; "Quantitative Analysis of Defects in Silicon", Quarterly Progress Report No. 4, DOE/JPL 954977, Materials Research, Inc., Technical Report: MRI-269, 1979.
2. Quantimet 720 Image Analysing Computer Operating Manual, 2nd Edition, Cambridge Instrument Company, Inc., November, 1971.
3. M. Leipold, R. De Angelis, "Structure Development in Silicon Sheet By Shaped Crystallization", Proceedings from the International Photovoltaic Solar Energy Conference, D. Reidel Publishing Company, 1978.
4. M. Leipold, R. Stirn, J. Zoutendyk and R. De Angelis, "Evaluation of Silicon Ribbon Material for Solar Cell Fabrication", Proceedings of the Eleventh IEEE Photovoltaic Conference, May, 1975.
5. L. C. Garone, C. V. Hari Rao, A. D. Morrison, T. Surek and R. V. Ravi, "Orientation Dependence of Defect Structure in EFG Silicon Ribbons", Applied Physics Letters, Vol. 29, 15 Oct. 1976.
6. R. J. De Angelis, "Structural Characterization of Edge-Defined Film Growth (EFG) Silicon Ribbon", unpublished report.

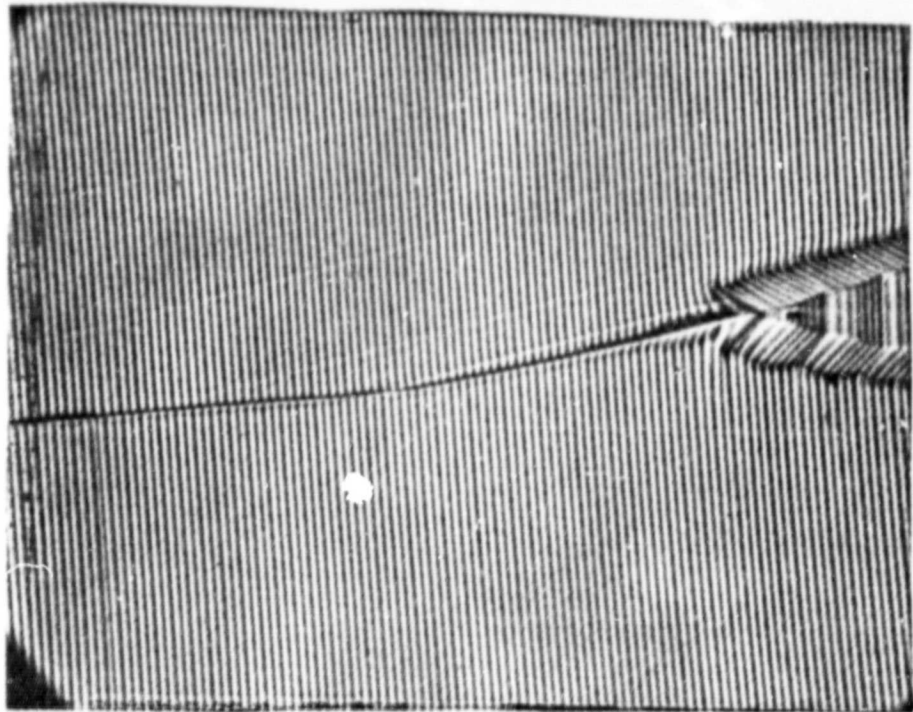


Figure 1. IBM #1-section 1-area 1, micrograph of silicon ribbon surface showing intersection of three grains after cleaning organic materials from surface of ribbon. Mag 200X

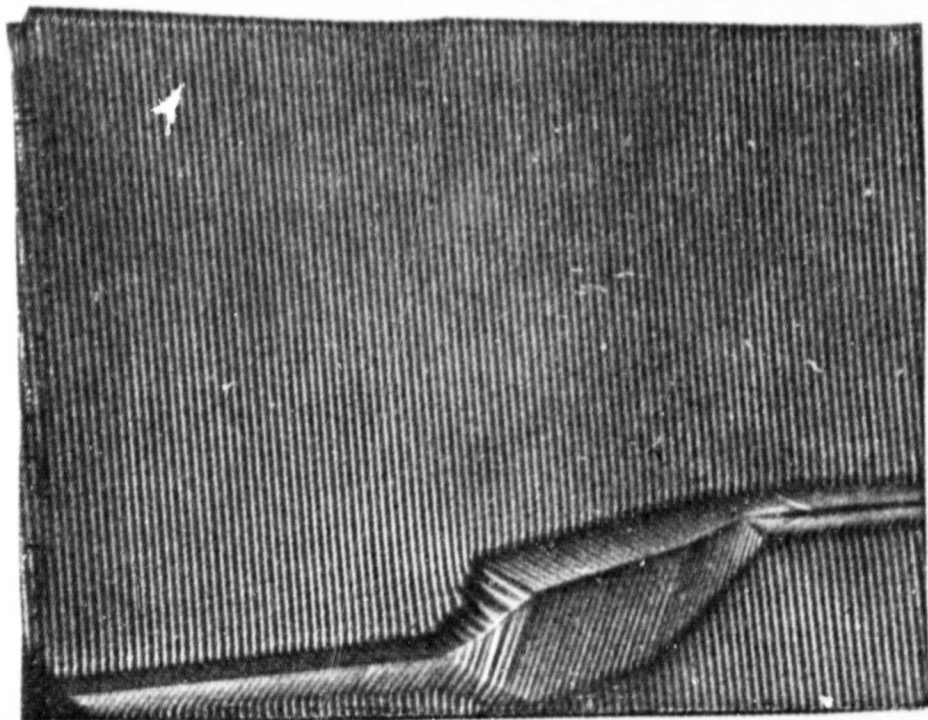


Figure 2. IBM #1-section 1-area 2, micrograph of ribbon surface showing grain boundaries after cleaning organic materials from surface of ribbon. Mag 200X

ORIGINAL PAGE IS
OF POOR QUALITY

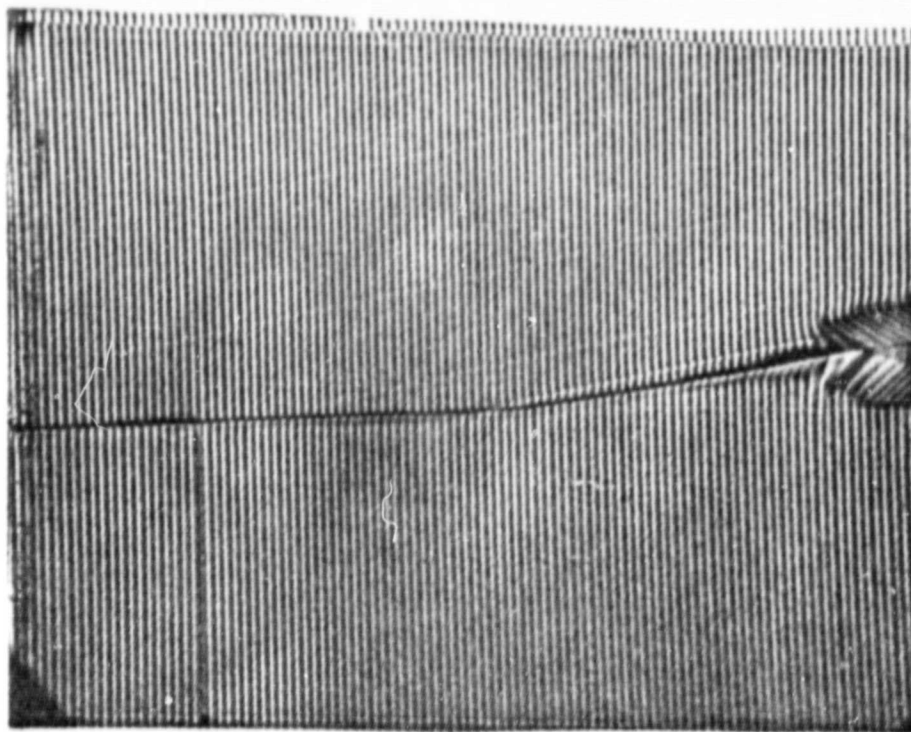


Figure 3. IBM #1-section 1-area 1, micrograph of ribbon surface, shown earlier in Fig. 1, after oxide removal. Mag 200X

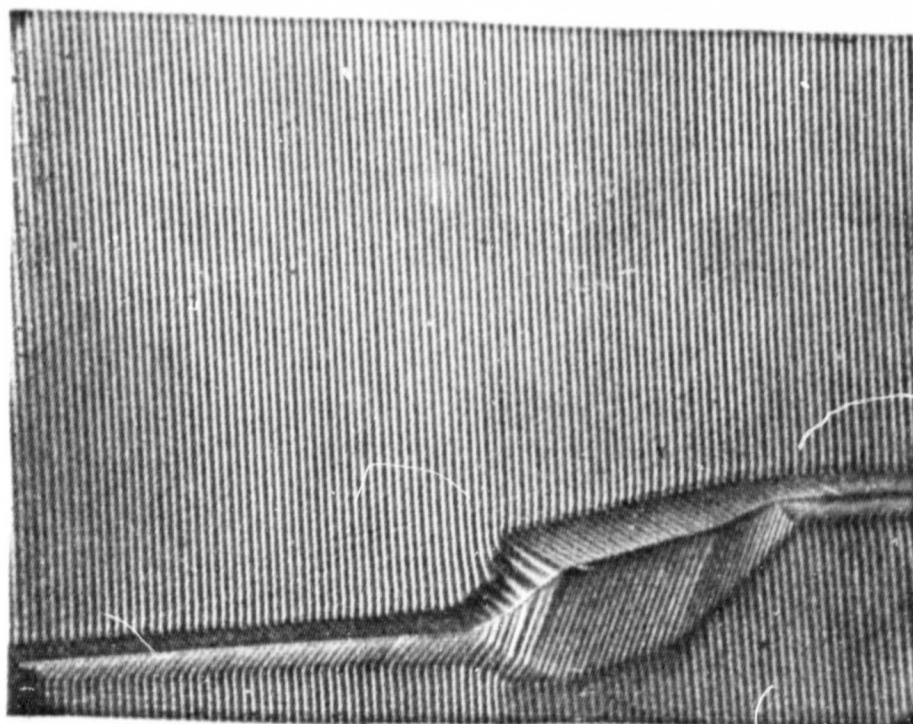


Figure 4. IBM #1-section 1-area 2, micrograph of ribbon surface, shown earlier in Fig. 2, after oxide removal. Mag 200X

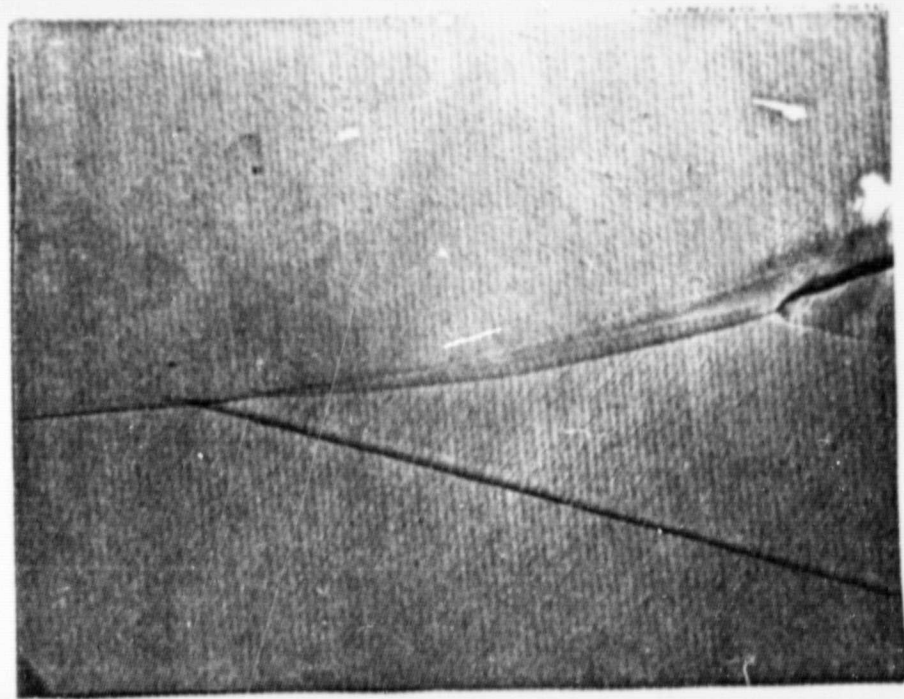


Figure 5. IBM #1-section 1- area 1, micrograph of ribbon surface, shown earlier in Fig. 1, after chemical polishing. Growth lines are removed and grain boundaries are revealed.

ORIGINAL PAGE IS
OF POOR QUALITY

Mag 200X

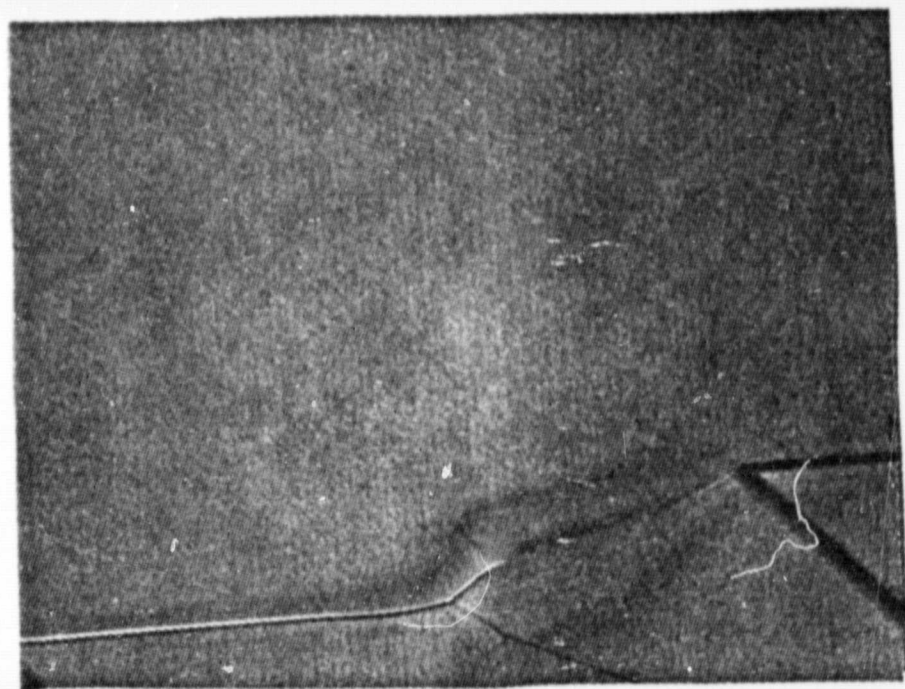


Figure 6. IBM #1-section 1- area 2, micrograph of ribbon surface, shown earlier in Fig. 2, after chemical polishing. Growth lines are removed and grain boundaries are revealed.

Mag 200X

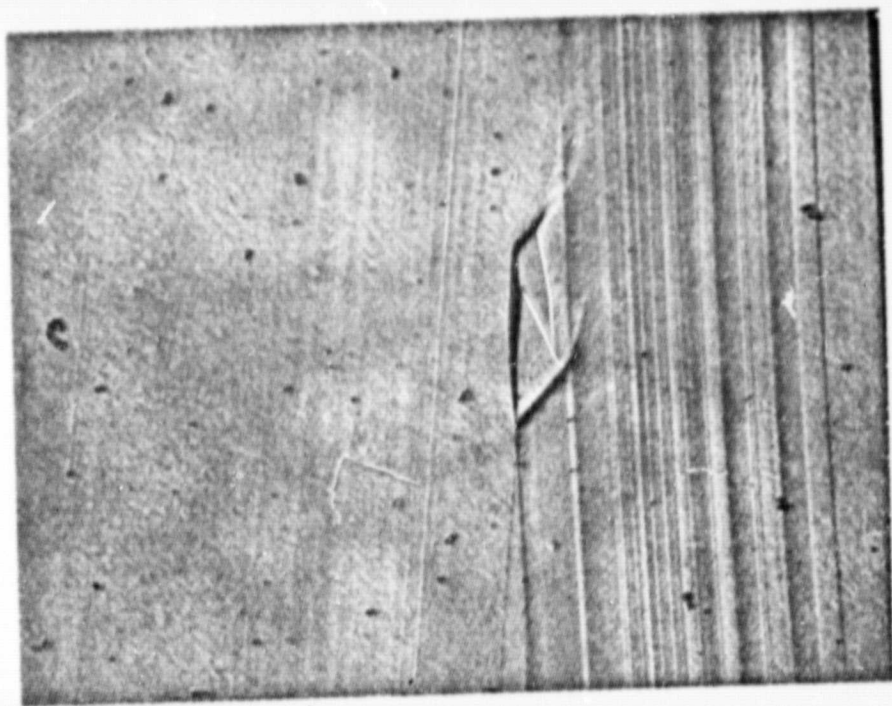


Figure 7. IBM #6 - Section 1 - Side 1, micrograph of ribbon surface after chemical polishing.
Mag 200X

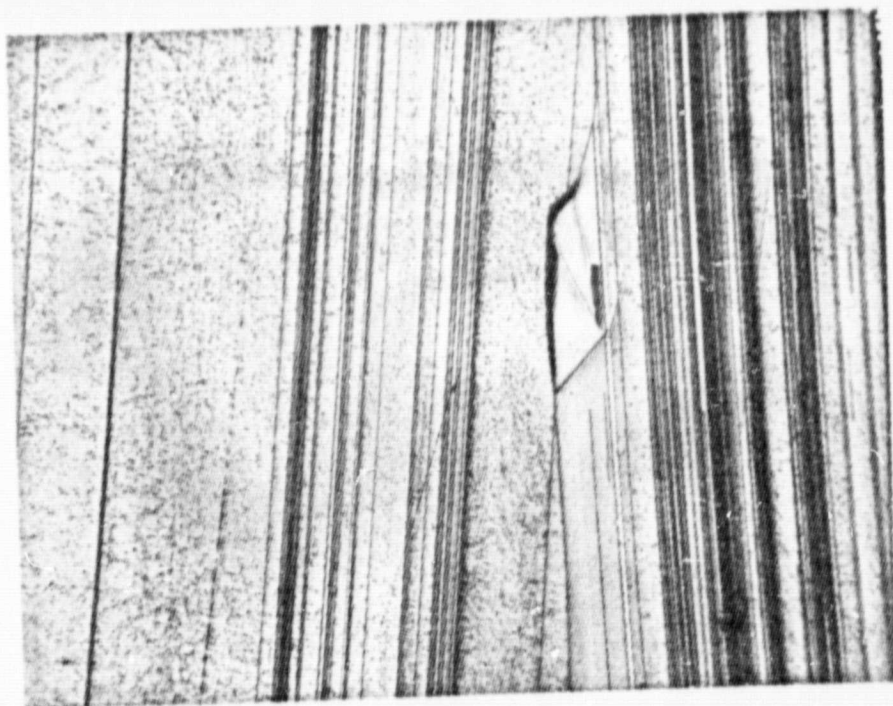


Figure 8. IBM #6 - Section 1 - Side 1, micrograph of ribbon surface after a 15 second etch by Etching Solution I
Mag 200X

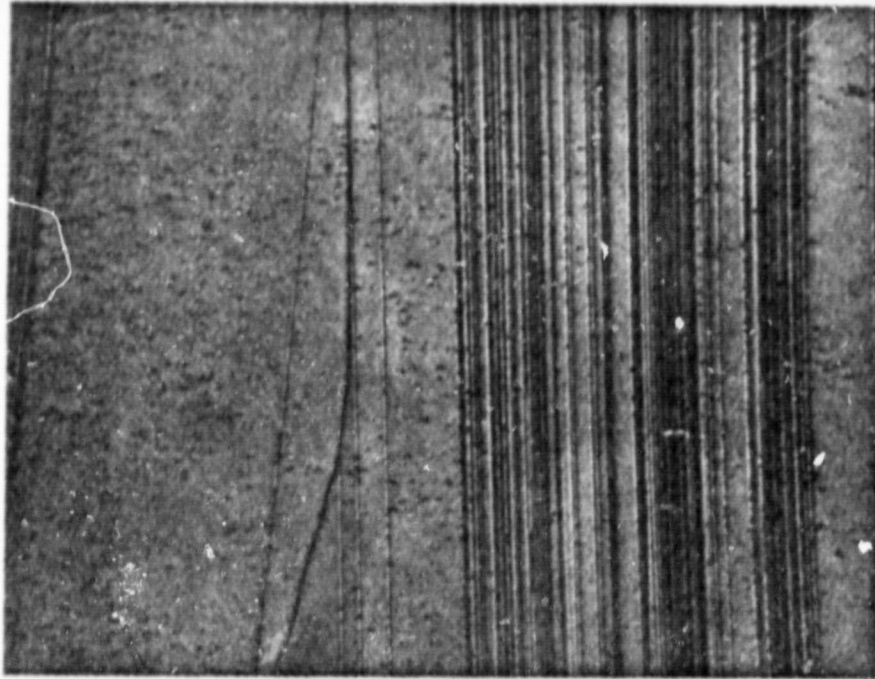


Figure 9. IBM #6 - Section 1 - Side 1, micrograph of ribbon surface after a 15 second etch by Etching Solution I.

Mag 500X

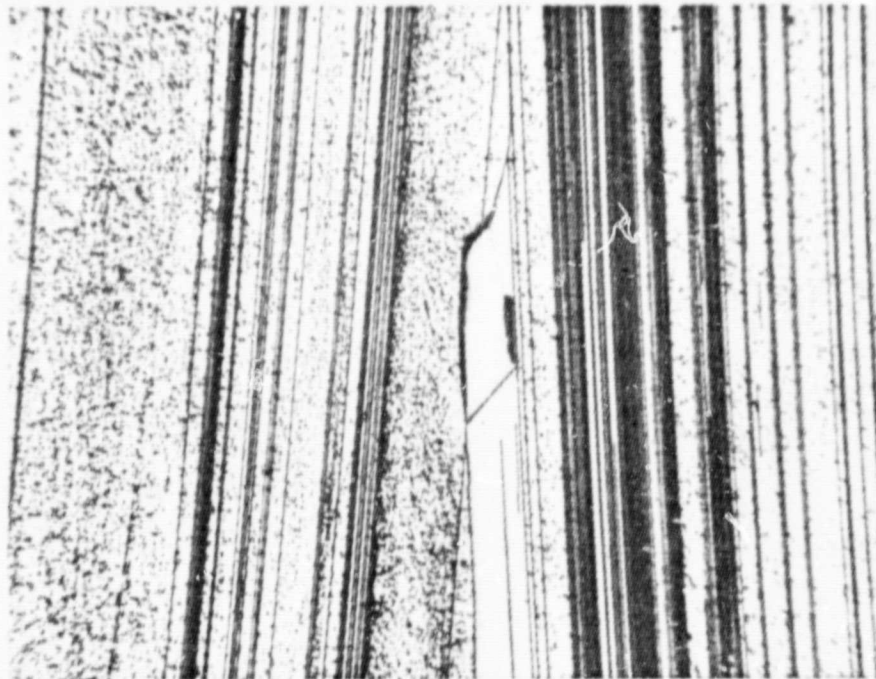


Figure 10. IBM #6 - Section 1 - Side 1, micrograph of ribbon surface, shown earlier in Fig. 7, 8 and 9, after a 30 second etch by Etching Solution I

Mag 200X

ORIGINAL PAGE IS
OF POOR QUALITY

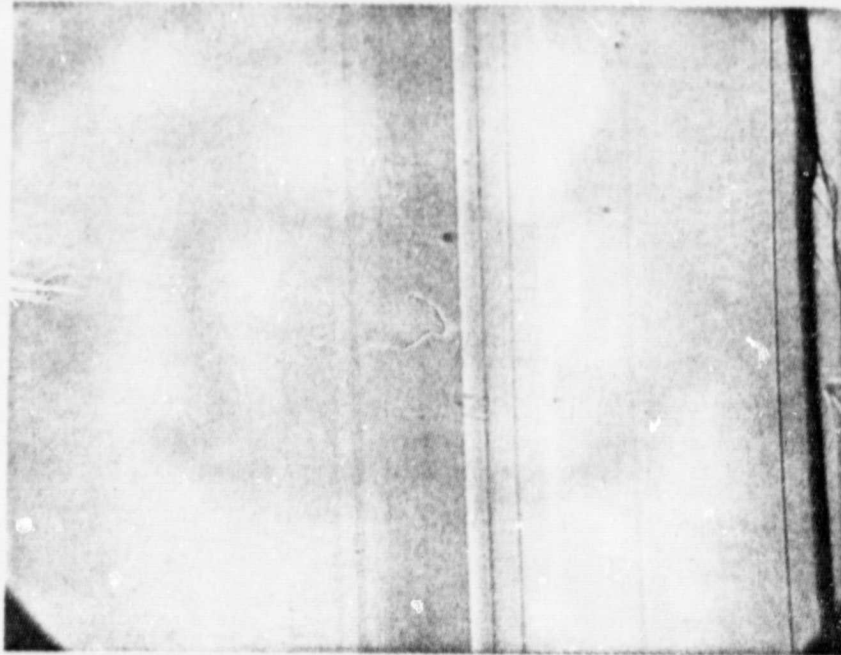


Figure 11. IBM #6 - Section 1 - Side 2, micrograph of ribbon surface after chemical polishing.
Mag 200X

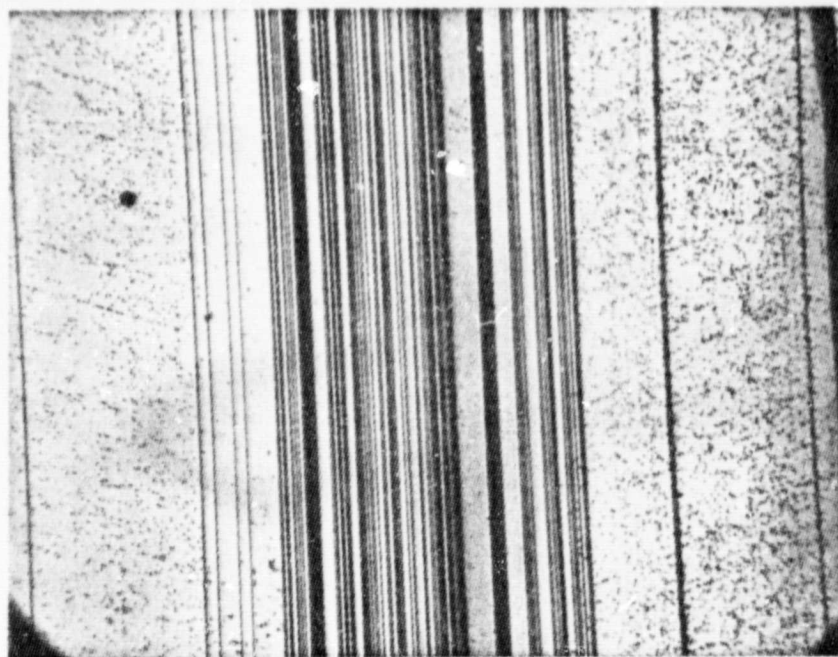


Figure 12. IBM #6 - Section 1 - Side 2, micrograph of ribbon surface, shown earlier in Fig. 11, after a 30 second etch by Etching Solution II.
Mag 200X

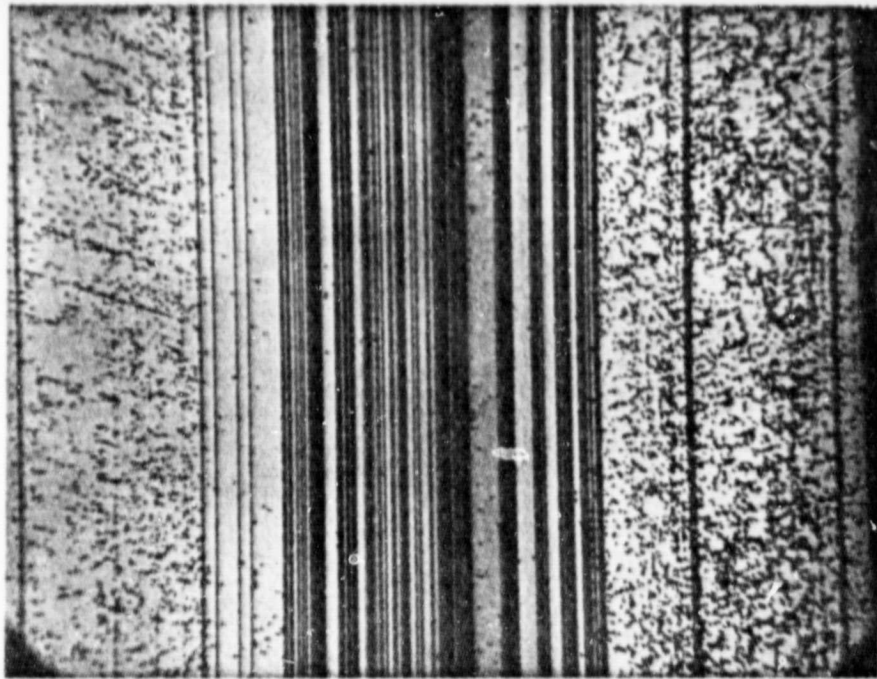


Figure 13. IBM #6 - Section 1 - Side 2, micrograph of ribbon surface, shown earlier in Figs. 11 and 12 after a 60 second etch by Etching Solution II.

Mag 200X

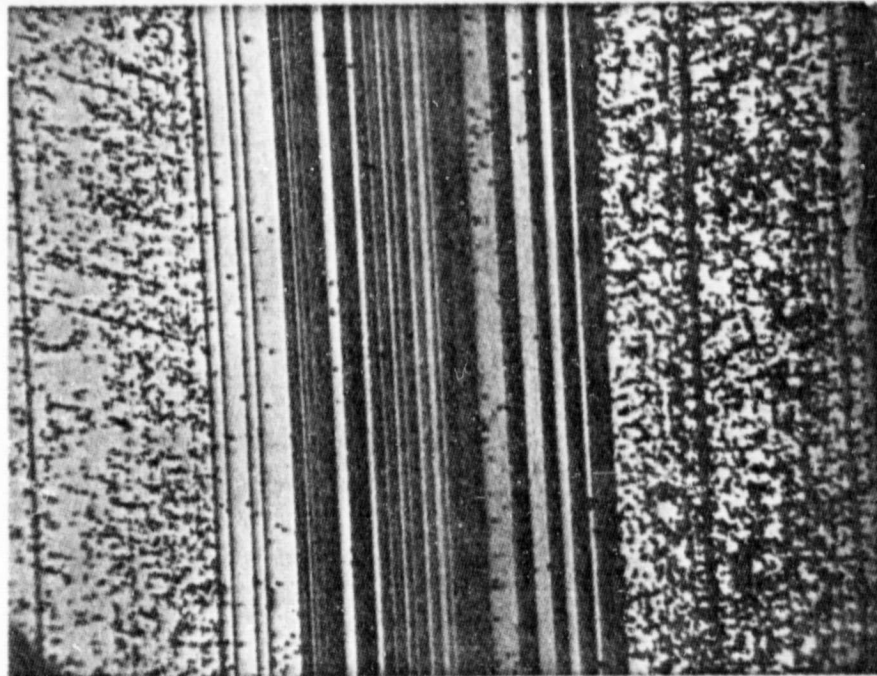


Figure 14. IBM #6 - Section 1 - Side 2, micrograph of ribbon surface, shown earlier in Figs. 11, 12, and 13 after a 90 second etch by Etching Solution II.

Mag 200X

ORIGINAL PAGE IS
OF POOR QUALITY

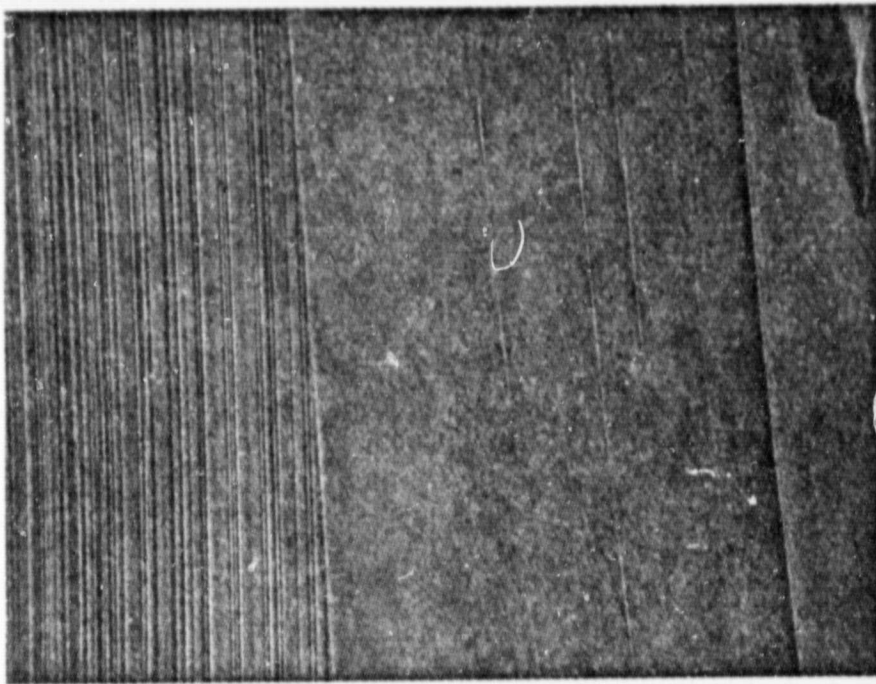


Figure 15. IBM #6 - Section 3 - Side 2 - Area 1,
micrograph of ribbon surface after chemical
polishing.

Mag 200X

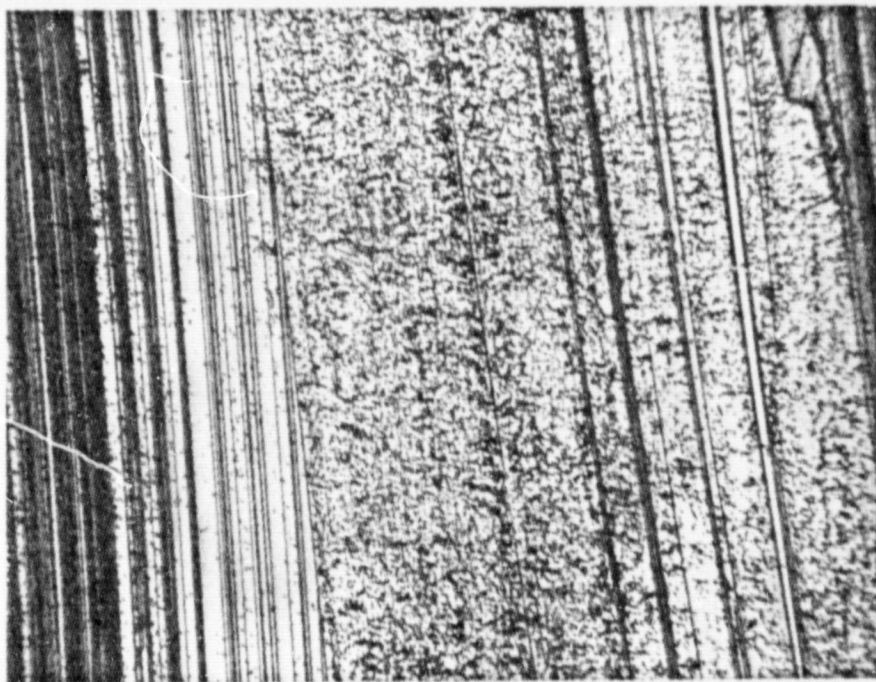


Figure 16. IBM #6 - Section 3 - Side 2 - Area 1, micrograph
of ribbon surface, as shown in Fig. 15, after a
60 second etch by Etching Solution III

Mag 200X

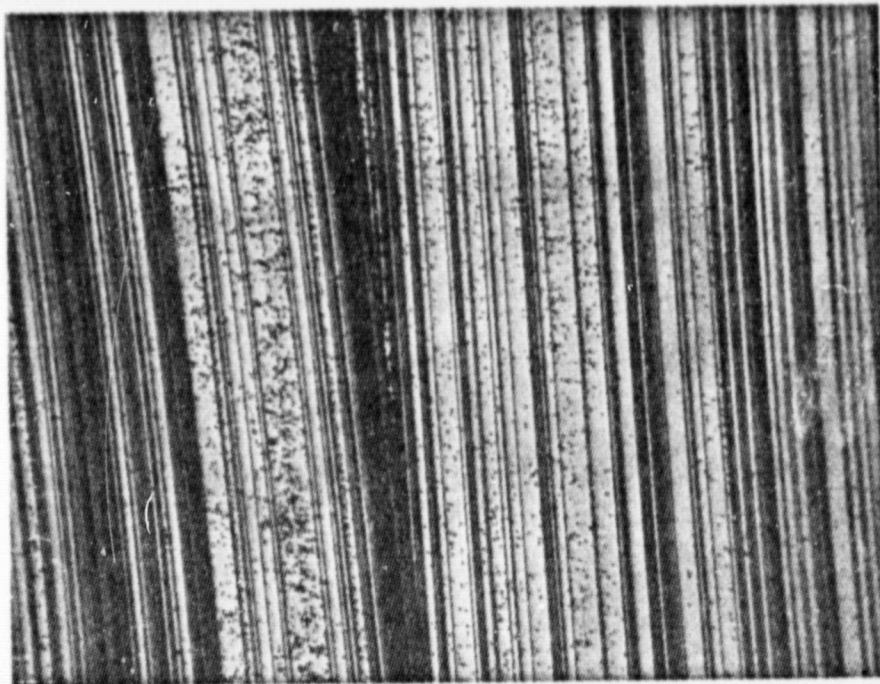


Figure 16A. IBM #6 - Section 3 - Side 2 - Area 2, micrograph of ribbon surface after a 60 second etch by Etching Solution III.

Mag 200X

ORIGINAL PAGE IS
OF POOR QUALITY

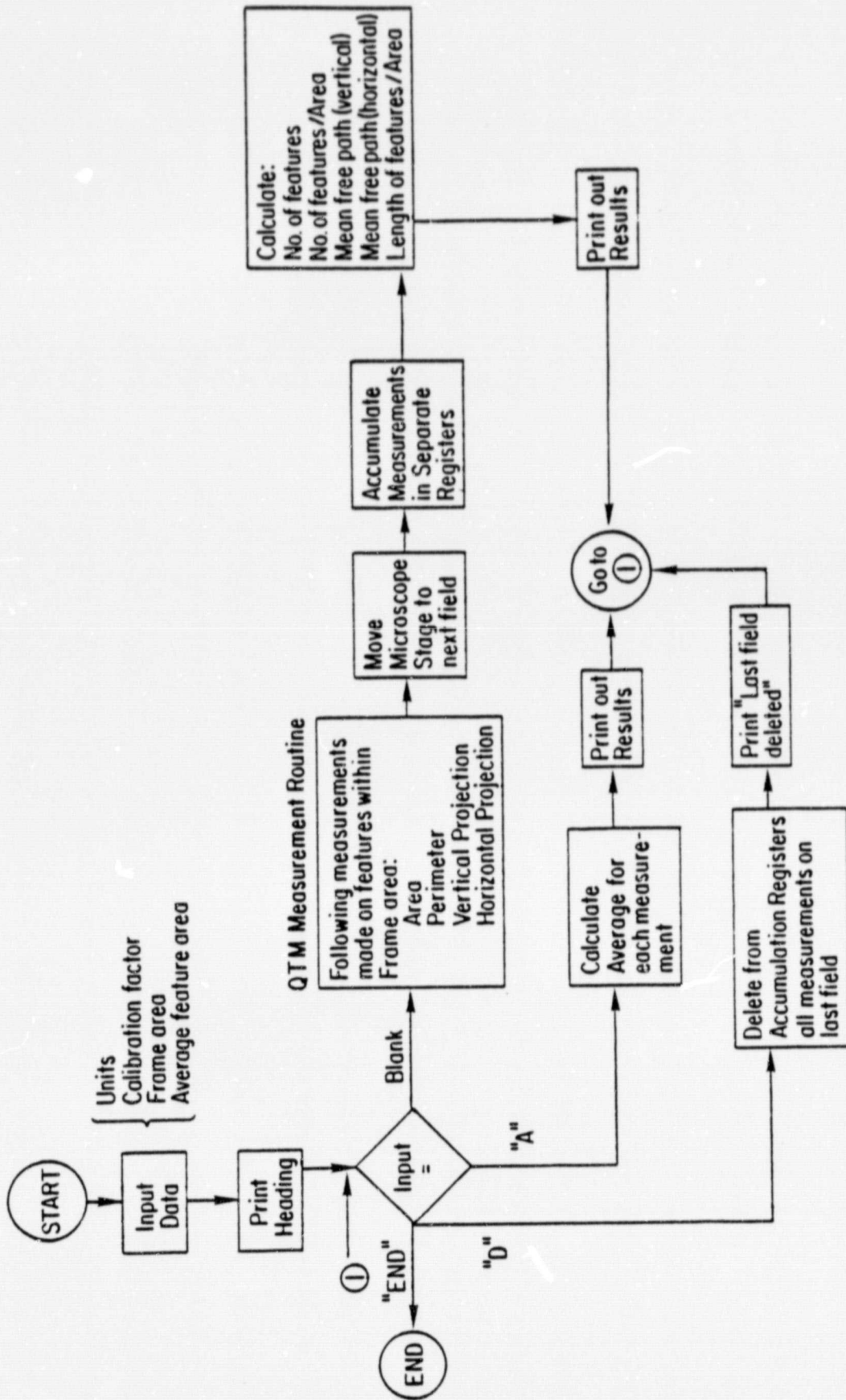


Figure 17. Flow Chart of BASIC Program for QTM Operation and Data Reduction.

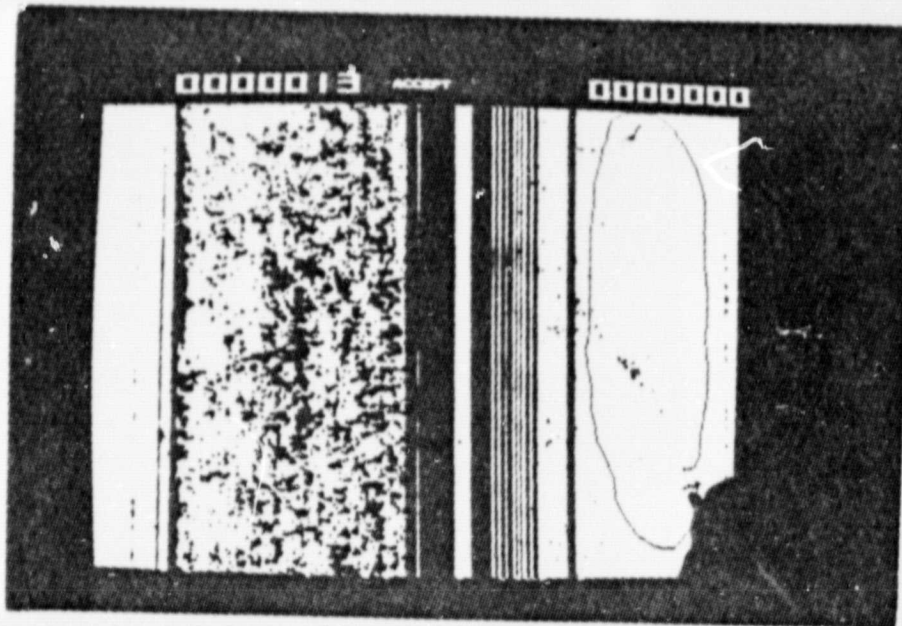


Figure 18A - Mobil Tyco # 53 - Field # 1
Photograph from QTM display screen
Mag. 800X

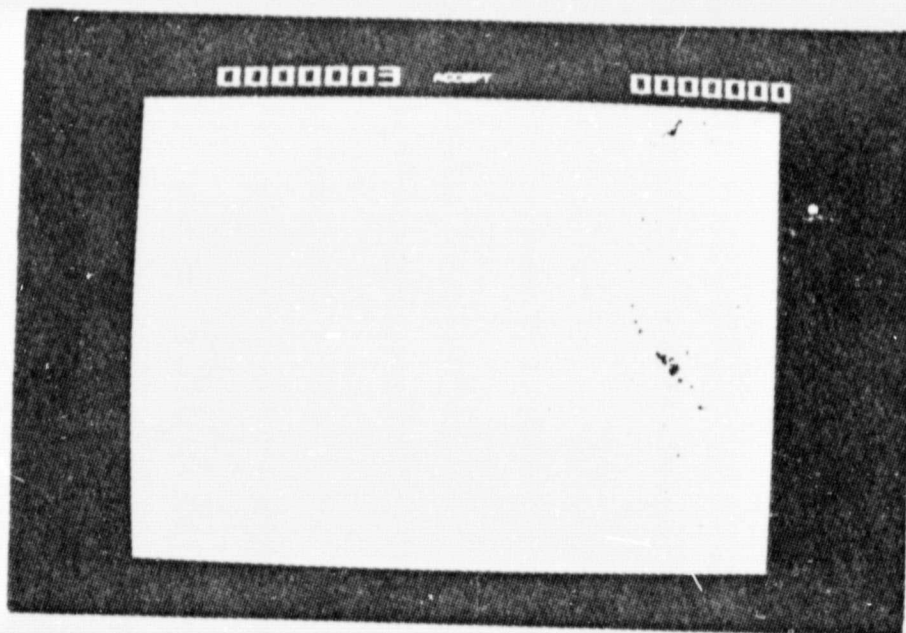


Figure 18B - Mobil Tyco # 53 - Field # 1
Photograph from QTM display screen showing only the
area of the sample that has been accepted.
Mag. 800X

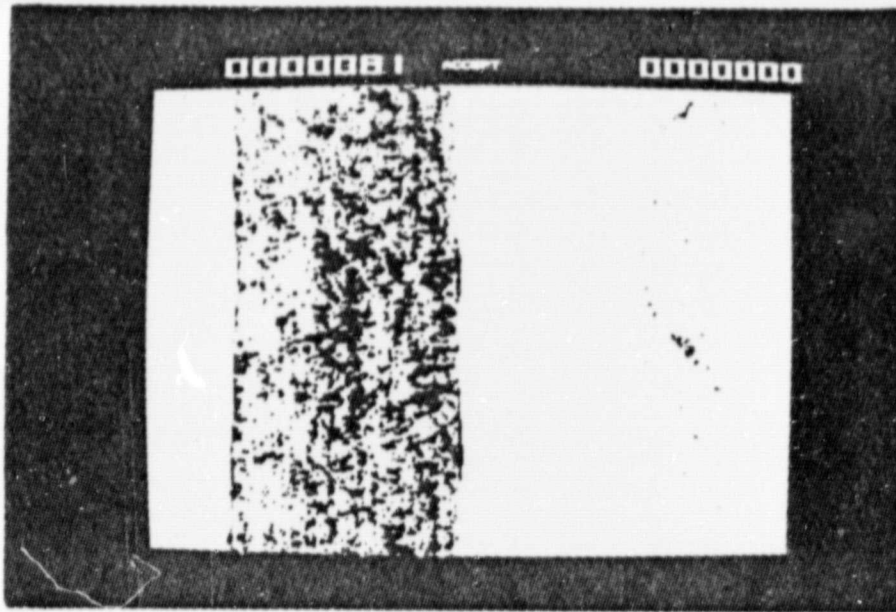


Figure 18C - Mobil Tyco # 53 - Field # 1
Photograph from QTM display screen showing dislocation
pits only. Mag. 800X

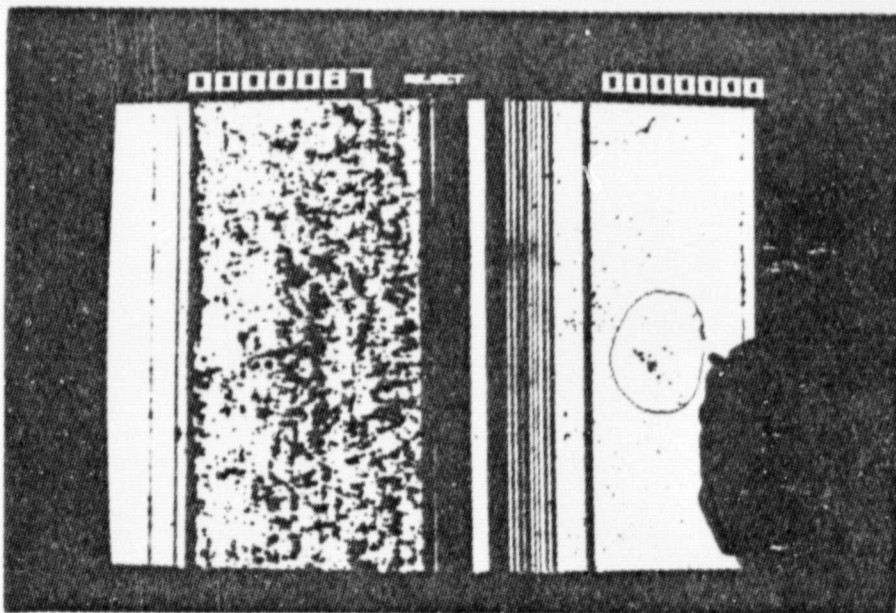


Figure 19A - Mobil Tyco # 53 - Field # 1
Photograph from QTM screen with an area being circled
by the light pen. Mag. 800X

ORIGINAL PAGE IS
OF POOR QUALITY

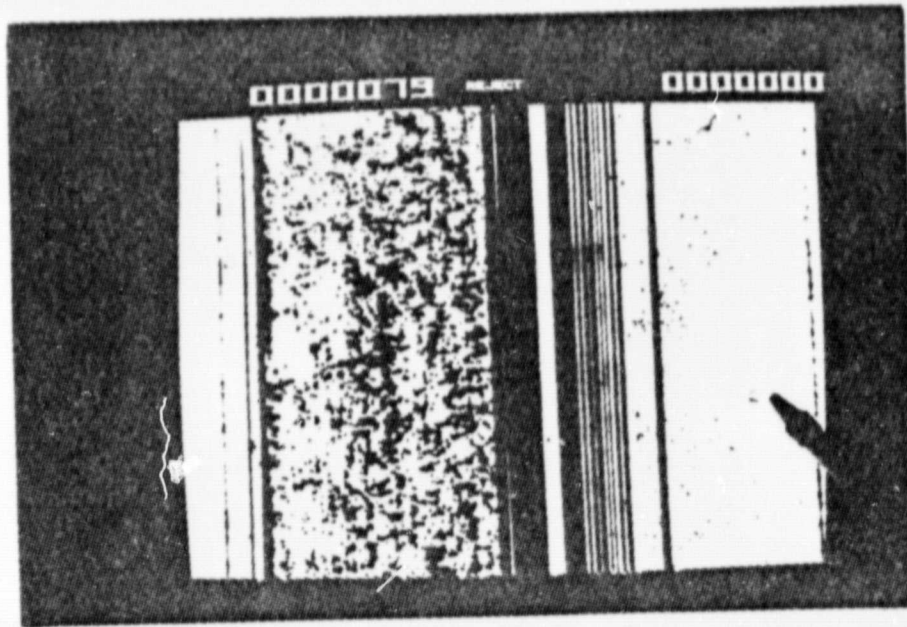


Figure 19B- Mobil Tyco # 53 - Field # 1
 Photograph from QTM display screen showing a small
 region that has been rejected.
 Mag. 800X

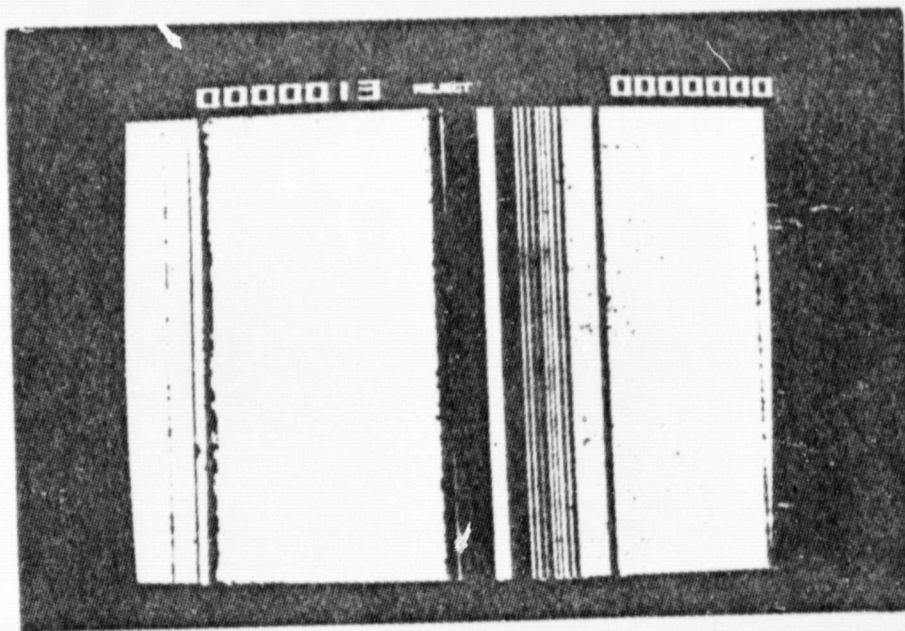


Figure 19C - Mobil Tyco # 53 - Field # 1
 Photograph from QTM display screen showing only the
 twins. The dislocation pits have been rejected.
 Mag. 800X



Figure 20A. Mobil Tyco # 53 - Field # 2
Photograph from QTM display screen showing an area
of dislocation pits with one twin boundary.
Mag. 800X

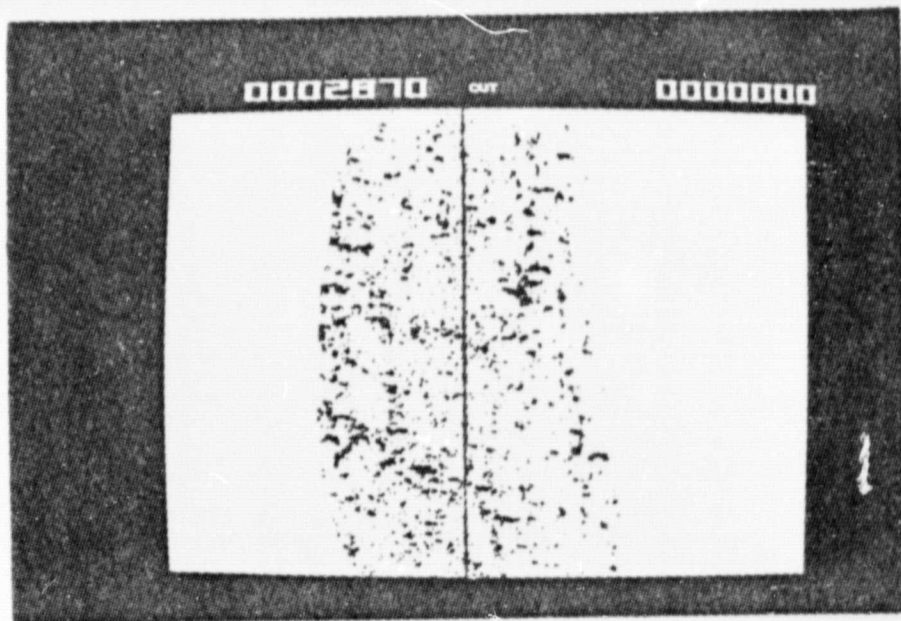


Figure 20B- Mobil Tyco # 53 - Field # 2
Photograph from QTM display screen showing the same
area as in Fig.20A. The twin has been separated from
the dislocation pits by use of the image editor.
Mag. 800X

IBM #1-7
JPL 4-457 Spec A-G

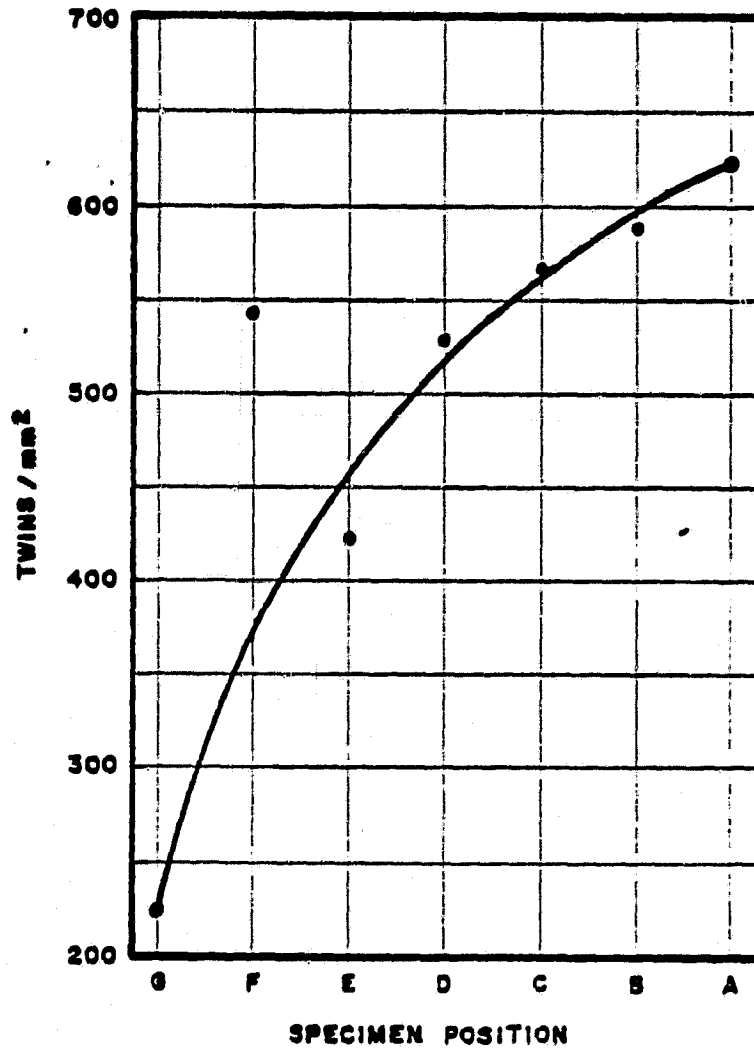


Fig. 21. Graphical plot showing systematic variation in twin density with respect to specimen location in IBM Ribbon No. 4-457.

MOBIL TYCO SAMPLES

NO. OF SAMPLES

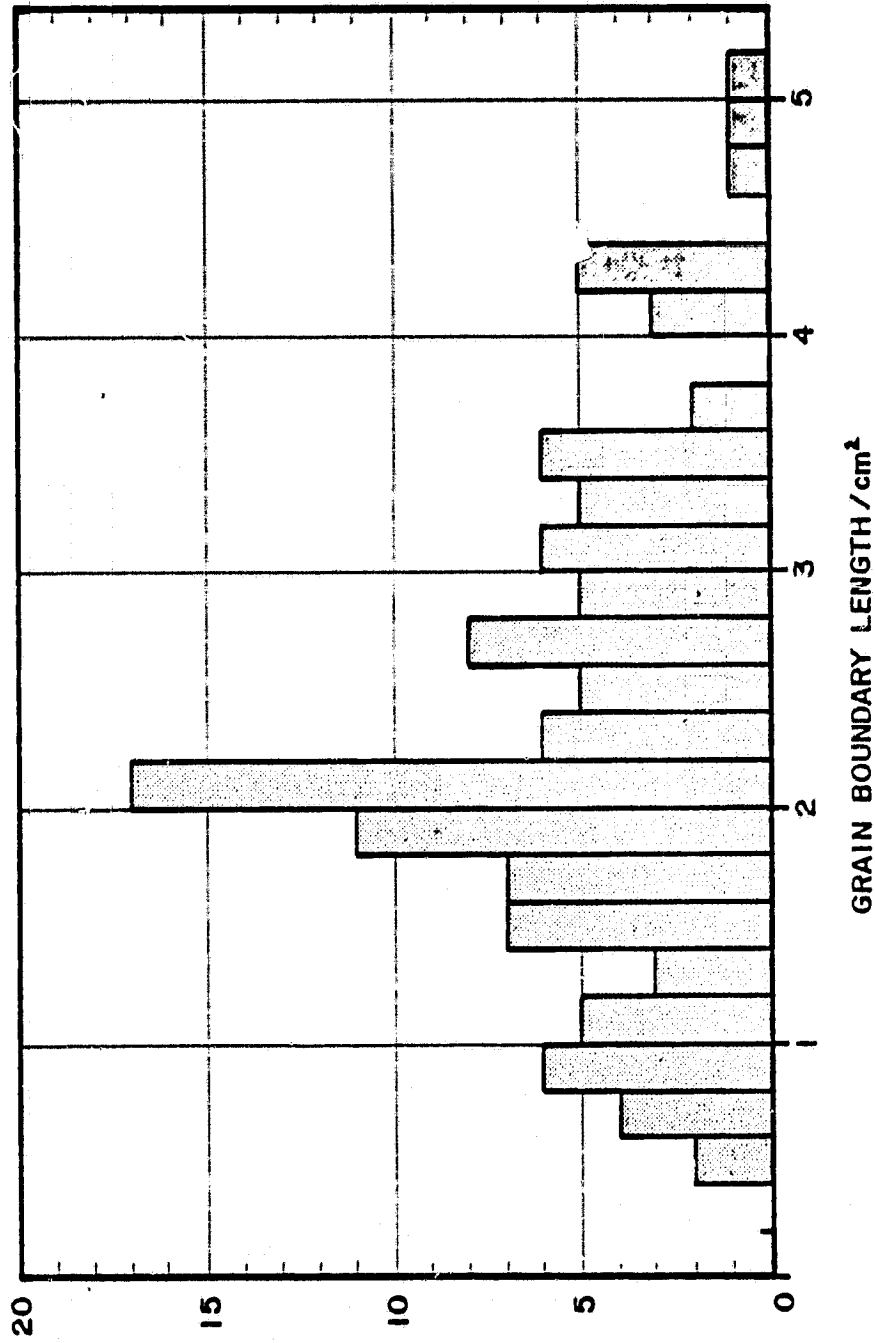


FIGURE 22

Histogram of grain boundary length of Mobil Tyco samples

MOBIL TYCO SAMPLES

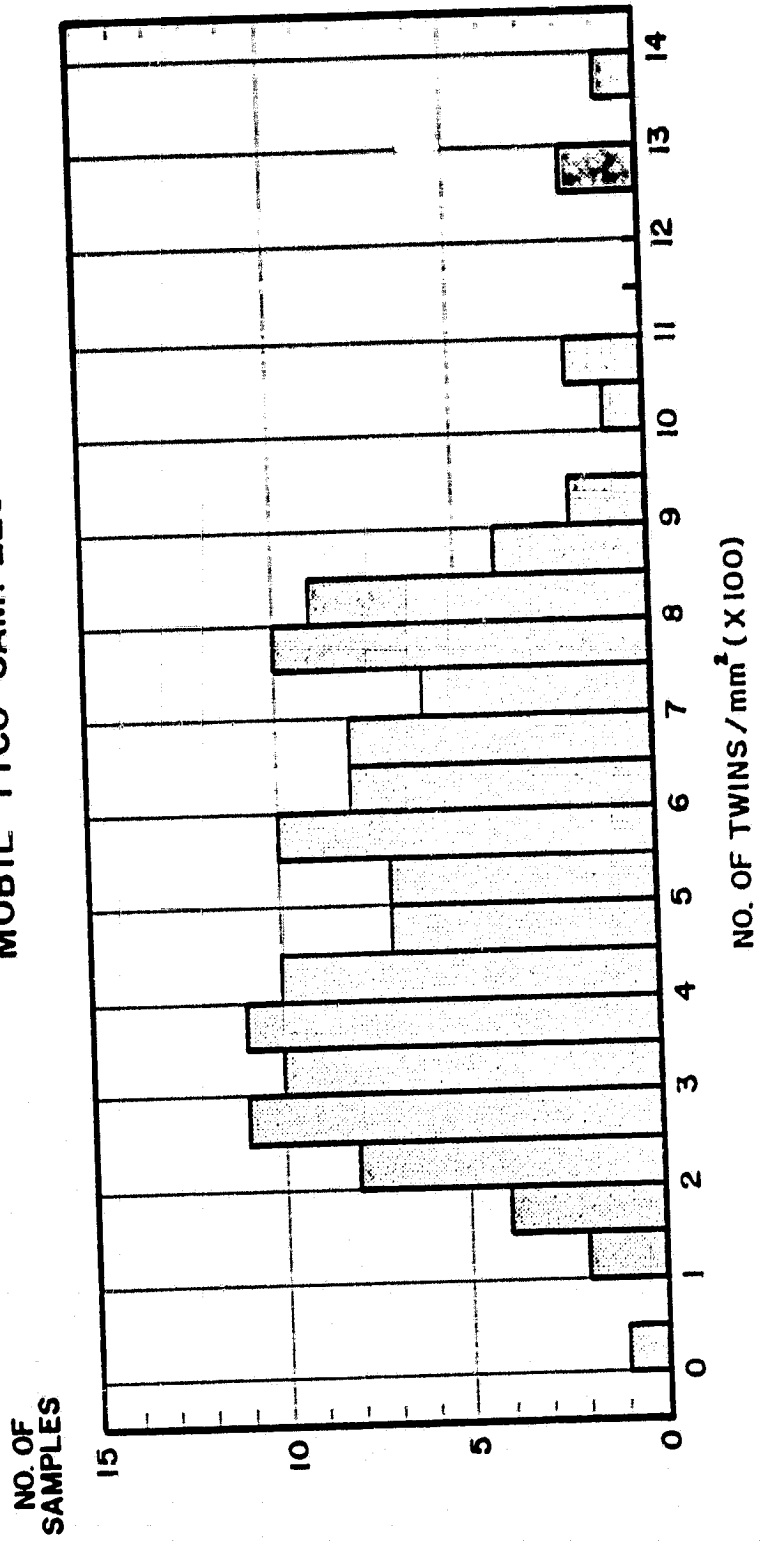


FIGURE 23

Histogram of twin boundary density of Mobil Tyco samples

MOBIL TYCO SAMPLES

NO. OF SAMPLES

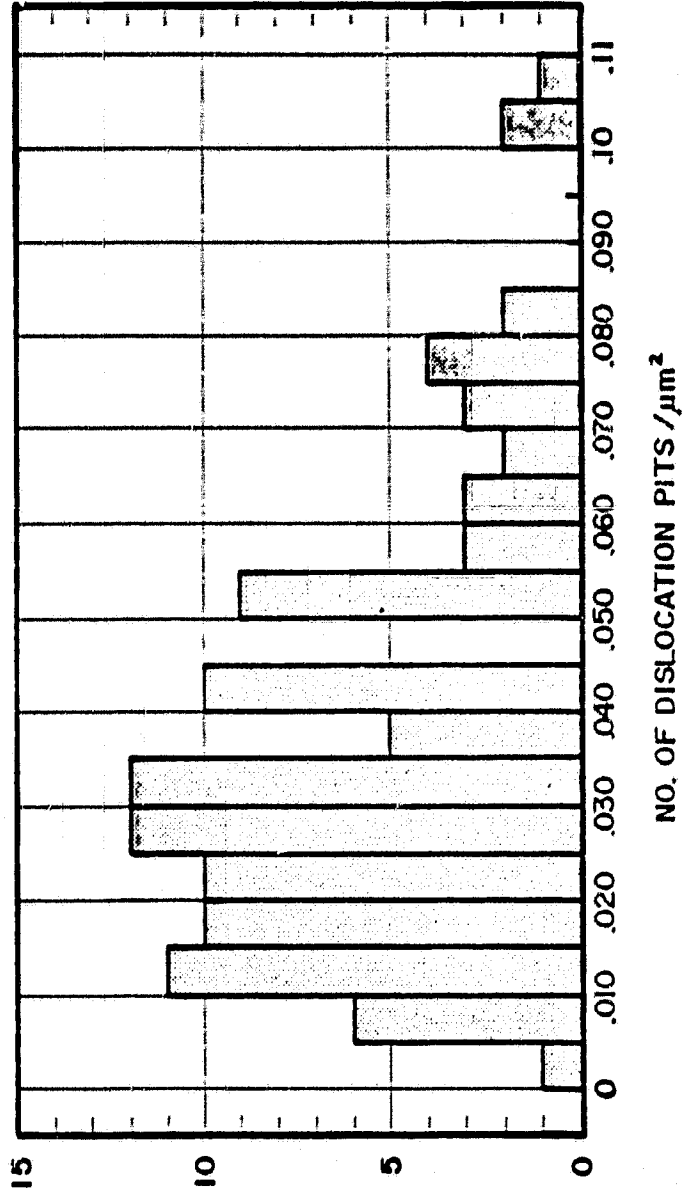


FIGURE 24

Histogram of dislocation pit density of Mobil Tyco samples

MOTOROLA SAMPLES

NO. OF SAMPLES

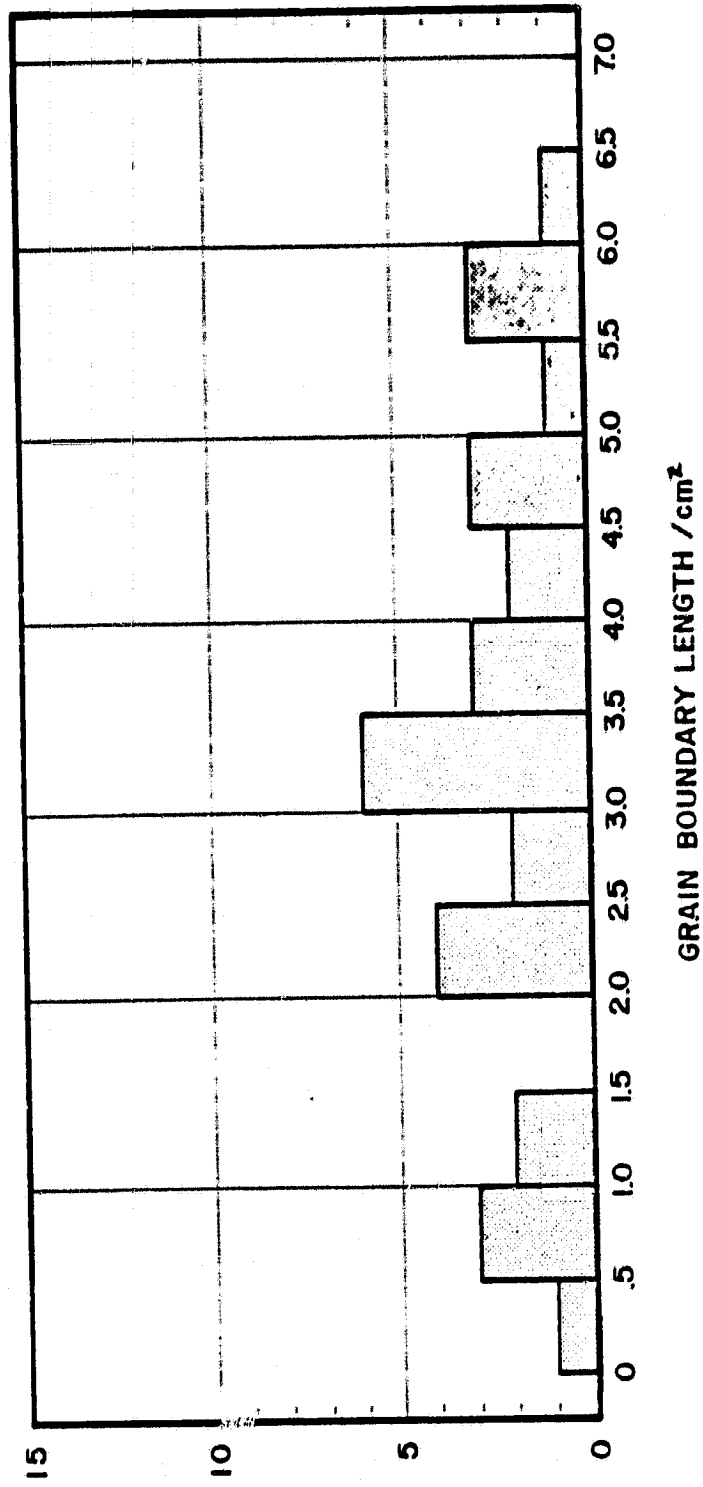


FIGURE 25

Histogram of grain boundary length of Motorola samples

MOTOROLA SAMPLES

NO. OF SAMPLES

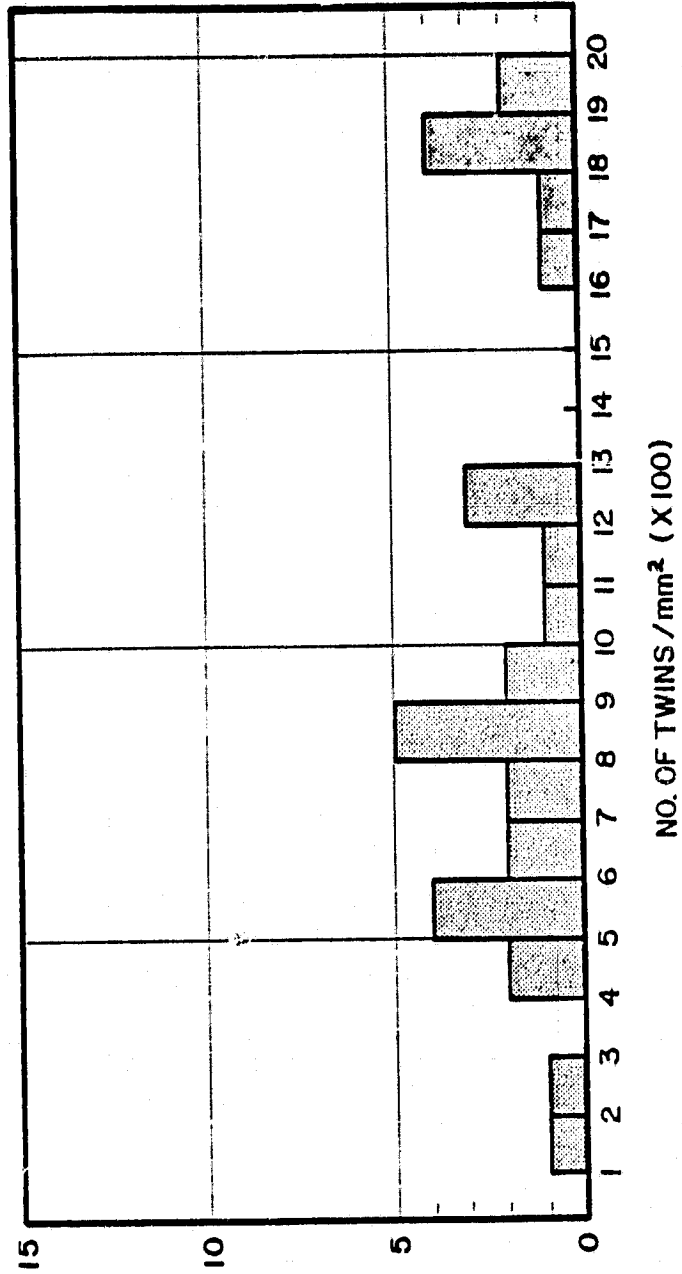
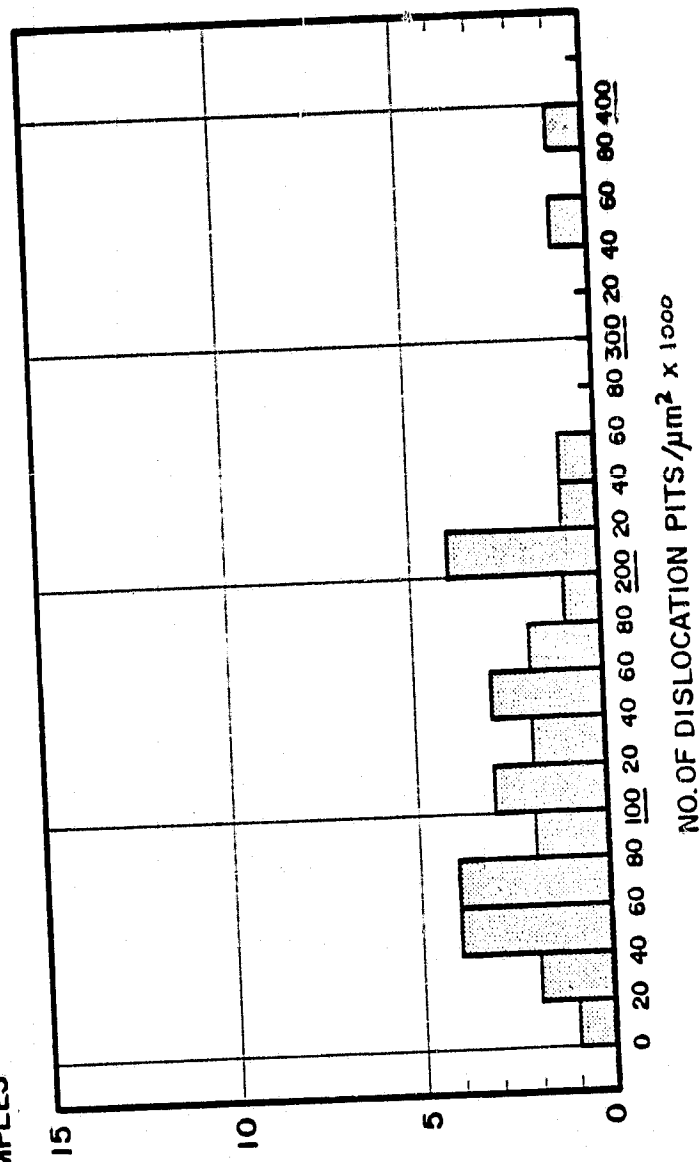


FIGURE 26

Histogram of twin boundary density of Motorola samples

MOTOROLA SAMPLES

NO. OF SAMPLES

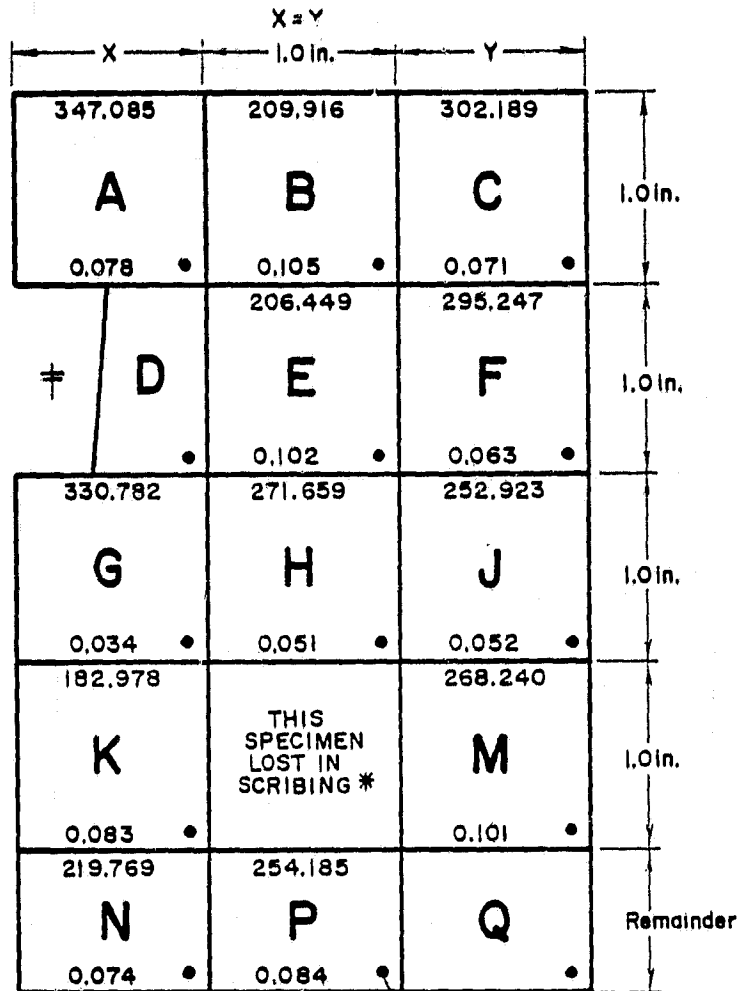


NO. OF DISLOCATION PITS/μm² x 1000

FIGURE 27

Histogram of dislocation pit density of Motorola samples

**MOBIL TYCO
RIBBON #5-685 (18-63-1)**



— ORIENTATION MARK
(SPOT OF INDELIBLE INK)
(TYPICAL 14 PLACES)

- * MOBIL TYCO 5-685 (18-63-1) SPEC. L LOST IN SCRIBING.
- ‡ THIS PORTION OF SPECIMEN D LOST IN SCRIBING.
- † SPEC. D MEASURED APPROX. 0.018 in thick.

Figure 28. Diagram showing the position of Mobil Tyco samples MRI # 19-30 as cut from ribbon 5-685. Twin density (per mm²) is printed at the top of each sample box, the dislocation density (per μm²) is printed at the bottom on each sample square.

**MOBIL TYCO
RIBBON 144-36, #5-742**

552.220	400.298	764.416	665.410
A	B	C	D
0.078 •	0.051 •	0.027 •	0.024 •
648.059	416.969	701.677	691.801
E	F	G	H
0.054 •	0.077 •	0.051 •	0.056 •

ORIENTATION MARK
(SPOT OF INDELIBLE INK)
(TYPICAL 8 PLACES)

**MOBIL TYCO
RIBBON 145-76, #5-744**

399.595	278.780	369.253	313.650
A	B	C	D
0.023 •	0.023 •	0.033 •	0.043 •
240.180	417.464	736.382	844.084
E	F	G	H
0.077 •	0.053 •	0.034 •	0.036 •

ORIENTATION MARK
(SPOT OF INDELIBLE INK)
(TYPICAL 8 PLACES)

Figure 29. Diagram showing the position of Mobil Tyco samples MRI # 31-46 as cut from ribbons 5-742 and 5-744.

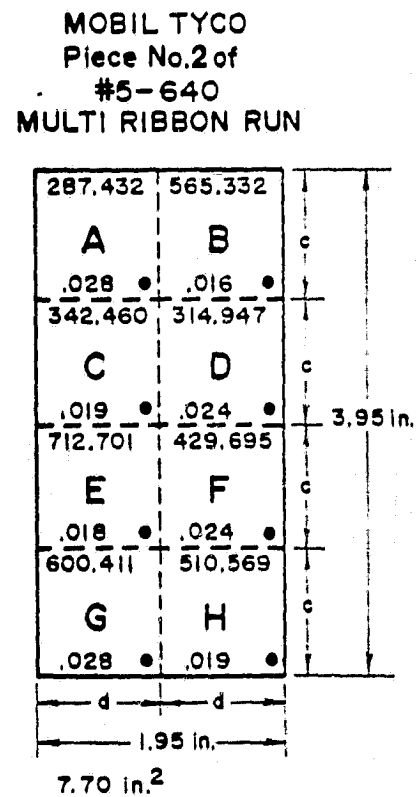
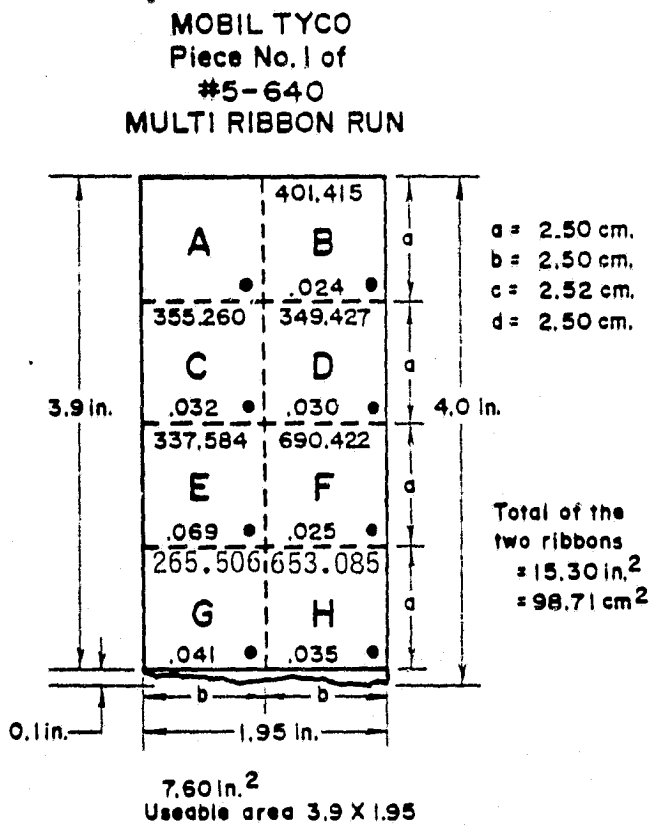
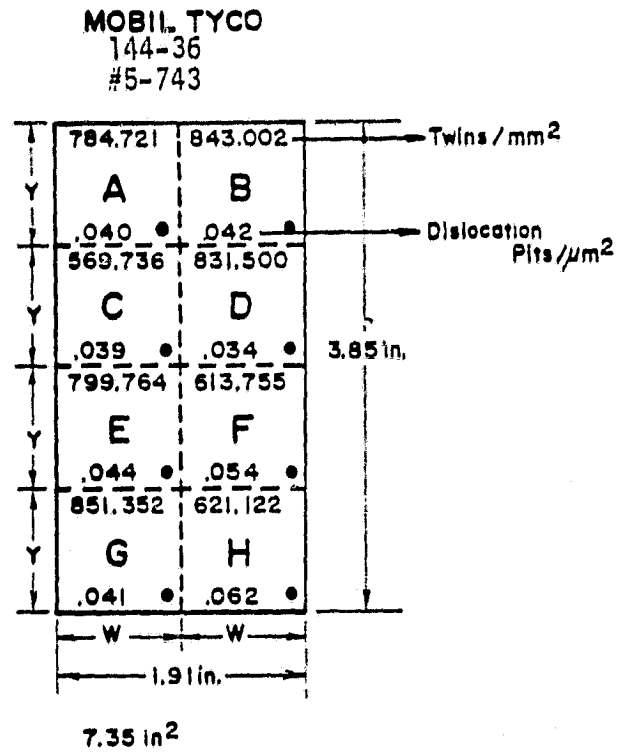
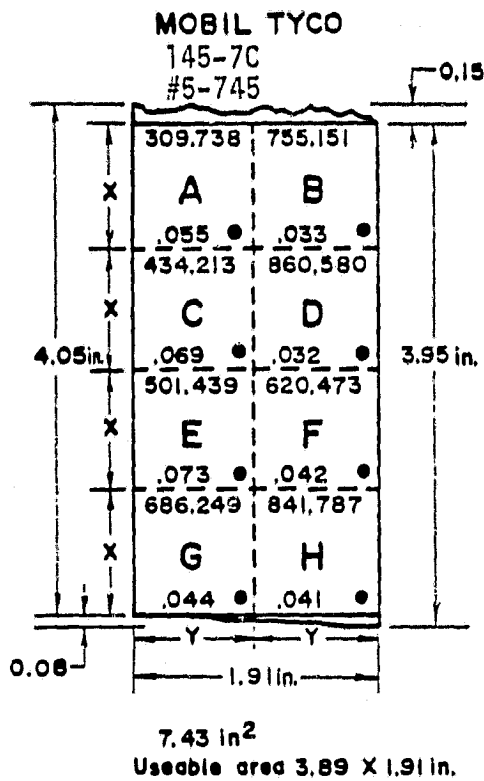


Fig. 30. Diagram showing the position of Mobil Tyco samples MRI #47-77 as cut from ribbons 5-745, 5-743, 5-640 #1 and 5-640 #2.

MOBIL TYCO
 SAMPLE #16-163-2
 JPL #5-867

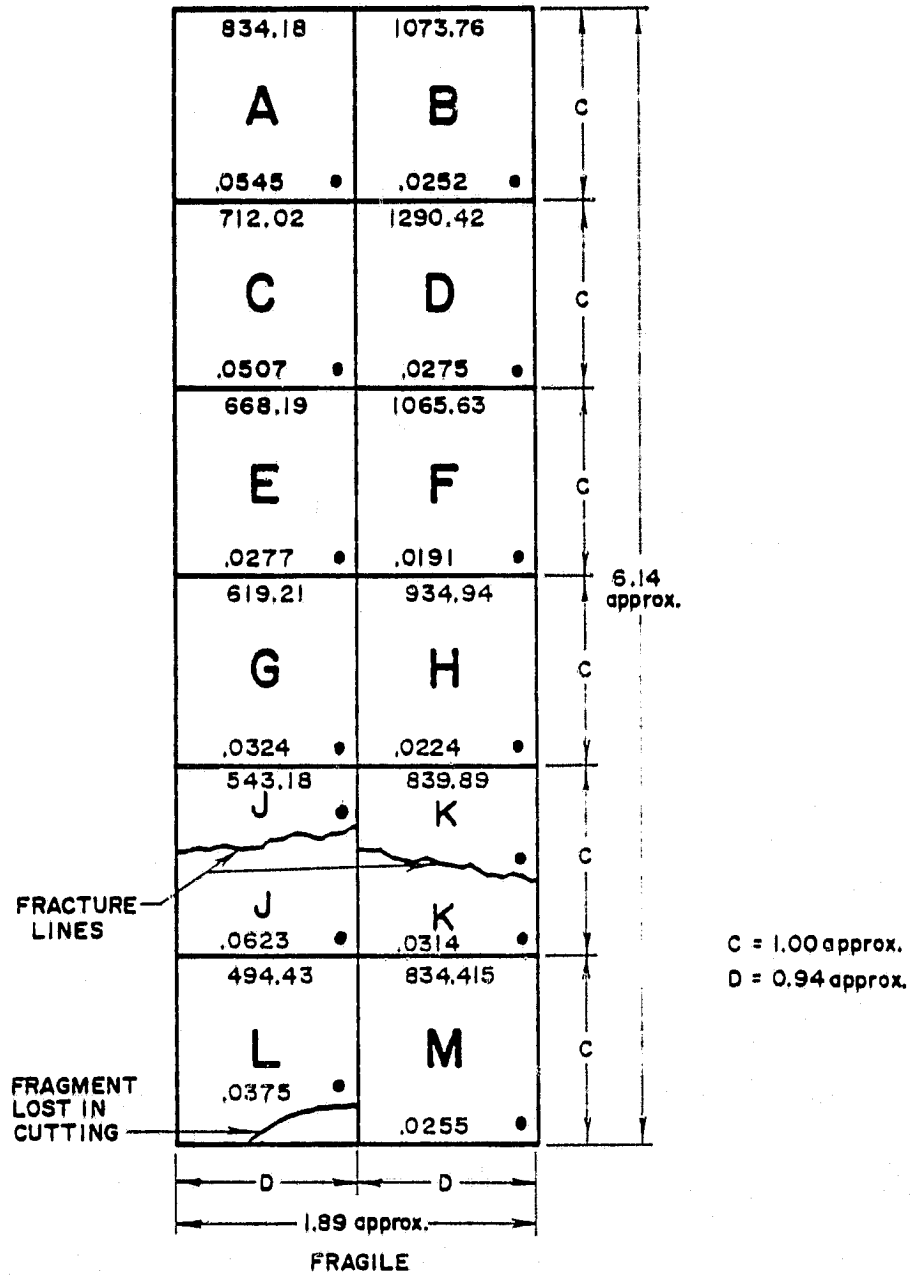


Figure 31. Diagram showing the position of Mobil Tyco samples MRI #78-90 as cut from ribbon 5-867.

MOBIL TYCO
JPL #5-640

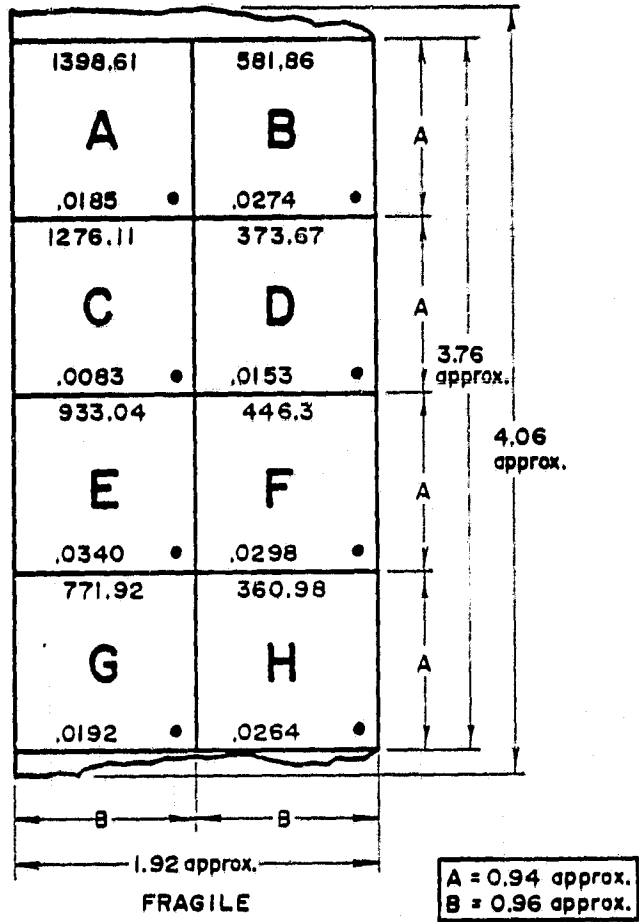
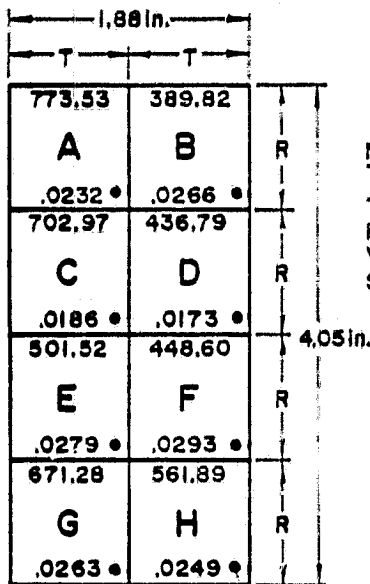


Figure 32. Diagram showing the position of Mobil Tyco samples MRI #91-98 as cut from ribbon 5-640.

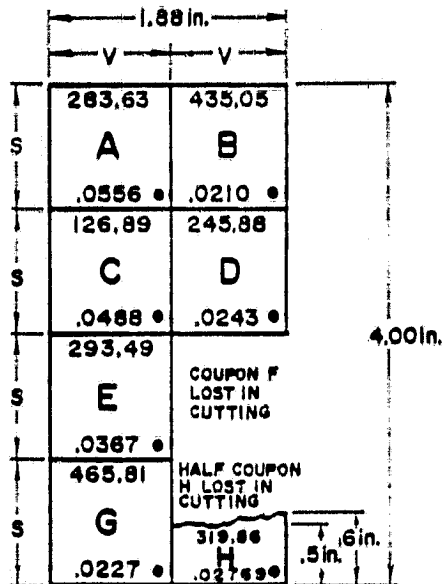
MOBIL TYCO
JPL #5-1092 EFG
RUN 16-187, STATION 1
SAMPLE 69



NOT DRAWN TO SCALE
T = approx. 0.94 in.
R = approx. 1.00 in.
V = approx. 0.94 in.
S = approx. 1.00 in.

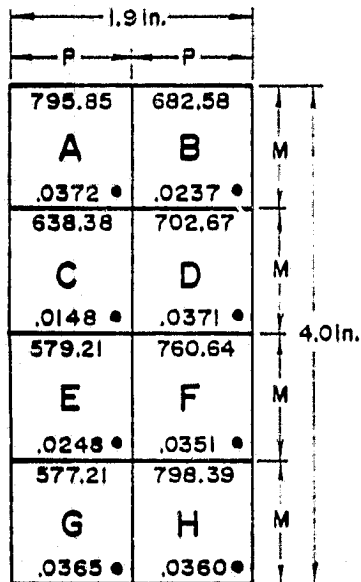
ORIENTATION MARK
(SPOT OF INDELIBLE INK)
(TYPICAL 8 PLACES)

MOBIL TYCO
JPL #5-1094 EFG
RUN 16-187, STATION 3
SAMPLE 33



ORIENTATION MARK
(SPOT OF INDELIBLE INK)
(TYPICAL 7 PLACES)

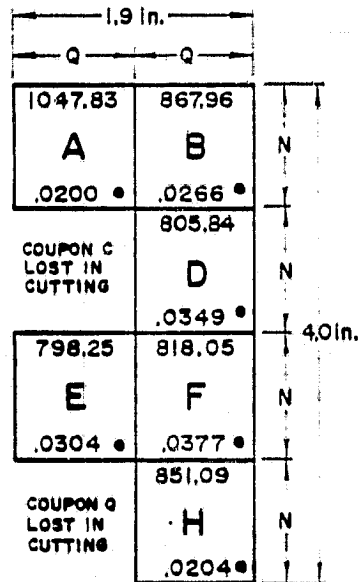
MOBIL TYCO
JPL #5-1063 EFG
RUN 16-184
SAMPLE 184-88 (Marked on package)
"184-225" MARKED IN INK ON SPECIMEN



NOT DRAWN TO SCALE
P = approx. 0.95 in.
M = approx. 1.00 in.
Q = approx. 0.95 in.
N = approx. 1.00 in.

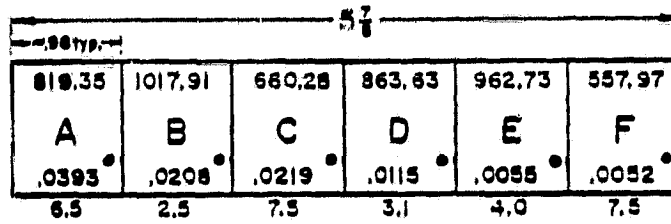
ORIENTATION MARK
(SPOT OF INDELIBLE INK)
(TYPICAL 8 PLACES)

MOBIL TYCO
JPL #5-1063 EFG
RUN 16-184
SAMPLE 184-175 (Marked on package)
"184-366" MARKED IN INK ON SPECIMEN

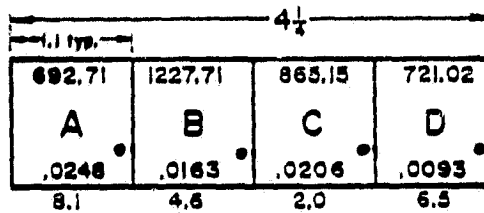


ORIENTATION MARK
(SPOT OF INDELIBLE INK)
(TYPICAL 6 PLACES)

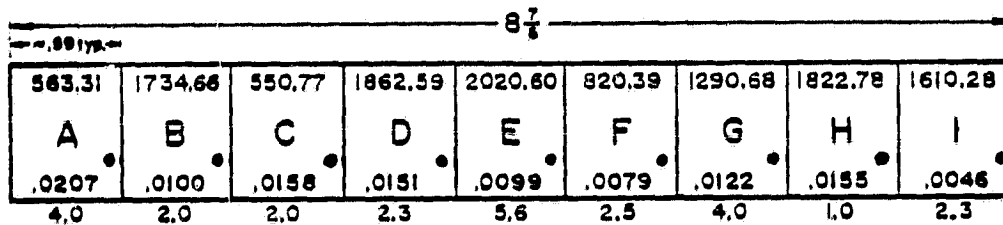
Figure 34. Diagram showing the position of Mobil Tyco samples MRI #106-134 as cut from ribbons 184-88, 184-175, 5-1094-33, and 5-1094-69



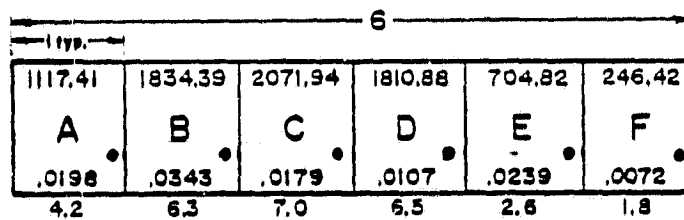
MOTOROLA
884-B
NO. 6-792



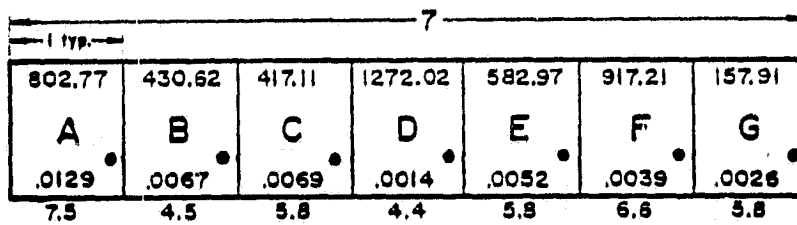
MOTOROLA
918-A
NO. 6-837



MOTOROLA
733-M
NO. 6-656



MOTOROLA
S 889-C
NO. 6-791



MOTOROLA
829-A
NO. 6-840

Figure 35. Diagram showing the position of Motorola samples MRI #1-32 as cut from ribbons 6-792, 6-837, 6-656, and 6-840.

Ribbon Identified as
IBM #4-457

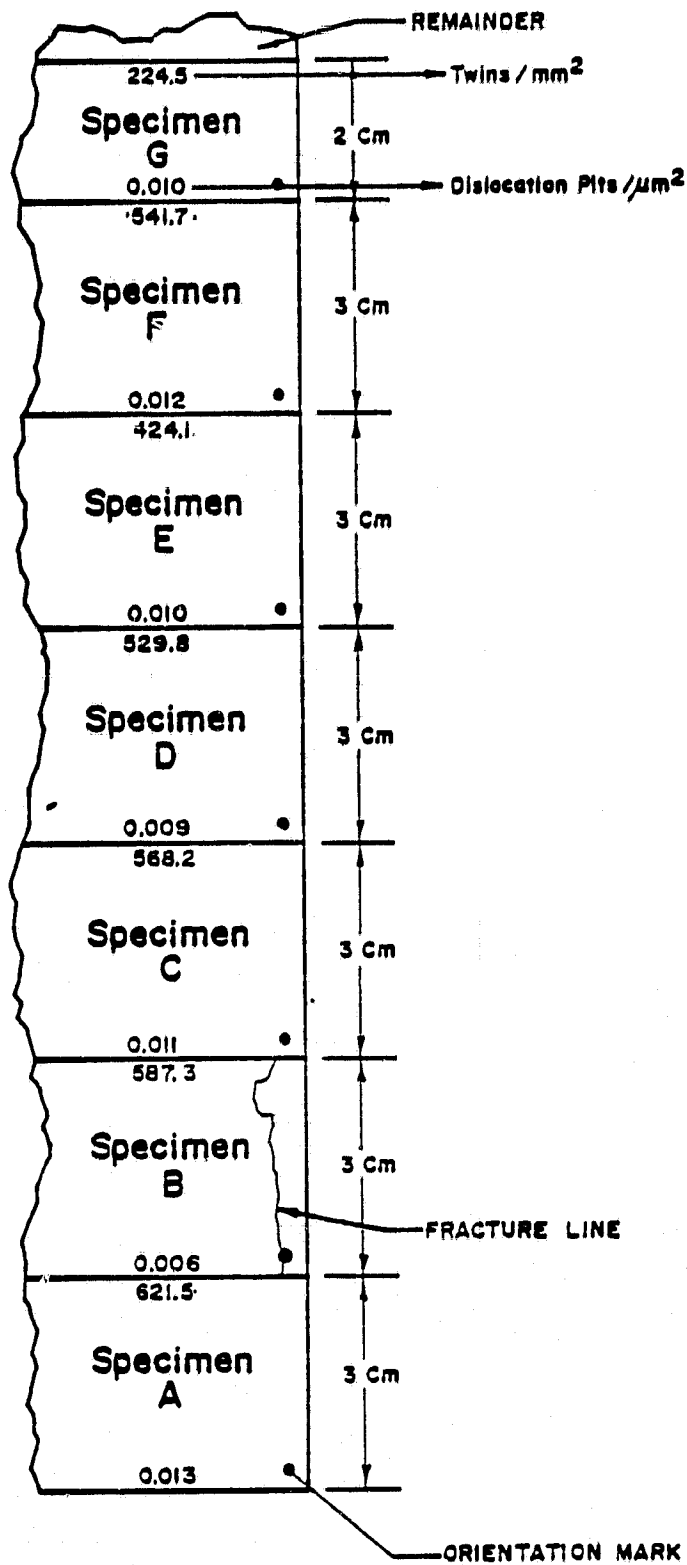


Figure 36. Diagram showing the position of IBM samples MRI #1-7 as cut from ribbon 4-457.

TABLE 1

CHEMICAL POLISHING OF WACKER SAMPLES

Polishing solution: mixture of HNO_3 : HF: CH_3COOH = 1: 2: 3 by volume

<u>Temperature ($^{\circ}\text{C}$)</u>	<u>Time (sec.)</u>	<u>Surface Conditions</u>
50	30	slight smoothening of surface; but no polishing
50	45	underpolishing of surface, growth lines remain.
50	60 to 75	slight underpolishing. Subgrain type structure (due to facets) becomes larger, and, in some places, becomes faint and starts disappearing. Get staining and pit formation inside subgrain type structure.
50	80 - 85	Good even polishing. Subgrain type structure, and pits within subgrains completely disappear.
70	45	slight underpolishing
80	55	reasonably good polish

- Note: (1) Time of polishing is to be increased or decreased depending on how soon and how fast bubbles evolve from sample surface.
- (2) For each polishing operation, a fresh solution must be used since the strength of solution decreases drastically after just one use.

TABLE 2

CHEMICAL POLISHING OF IEM SAMPLES

Polishing solution: mixture of HNO_3 : HF: CH_3COOH = 1: 2: 3 by volume

<u>Temperature (°C)</u>	<u>Time (sec.)</u>	<u>Surface Condition</u>
50	30	growth lines persist. Faceting persists.
50	45	growth lines disappear, but facets join together to form subgrain type structure.
50	60	surface appears very even and bright, however, faint remnants of subgrain type structure still persists.
50	85 to 90	Good even polishing

- Notes: (1) Time of polishing is to be increased or decreased depending on how soon and how fast bubbles evolve from sample surface.
- (2) For each polishing operation, a fresh solution must be used since the strength of solution decreases drastically after just one use.

T A B L E 3

CHEMICAL POLISHING OF MOTOROLA SAMPLESPolishing solution: mixture of HNO_3 :HF: CH_3COOH = 1:2:3 by volume

Temperature ($^{\circ}\text{C}$)	Time (Sec.)	Surface Condition
50	30	Growth lines persist. Sub-grain type structures present
50	35-45	Good even polishing
50	50	Faceting develops

T A B L E 4

CHEMICAL POLISHING OF MOBIL TYCO SAMPLES

Polishing solution: mixture of HNO_3 :HF: CH_3COOH = 1:2:3 by volume

Temperature ($^{\circ}\text{C}$)	Time (Sec.)	Surface Condition
50	30	Growth lines persist. Sub-grain type structures present
50	40	Good even polishing
50	50	Faceting develops

T A B L E 5

ANALYSIS OF MOBIL TYCO SAMPLES# M-5-738

Sample No. MRI	Average No. of Twins/field	Average No. of Twins/mm ²	No. of grain Boundaries	Average No. of dislocations/field	Average No. of dislocations/ μm^2
1	18.0	261.2	5	362.6	0.010
2	26.0	368.5	2	698.6	0.020
3	31.8	451.9	2	411.4	0.012
4	13.1	186.8	5	256.3	0.007
5	14.6	207.9	6	387.8	0.011
6	1.3	18.4	6	485.3	0.014
7	9.7	137.7	5	505.8	0.014
8	16.7	238.1	8	495.4	0.014
9	24.6	350.3	0	401.0	0.011
10	15.8	224.7	7	368.0	0.010
11	32.8	466.1	4	250.4	0.007
12	13.2	188.0	4	578.1	0.016
13	27.2	387.0	1	353.6	0.010
14	39.6	563.3	0	143.2	0.004
15	27.0	384.0	7	227.6	0.006
16	33.0	470.0	4	197.1	0.006
17	34.5	490.5	1	214.1	0.006
18	11.4	162.2	4	503.7	0.014

T A B L E 6.

ANALYSIS OF MOBIL TYCO SAMPLES

MRI Sample # (Mobil Tyco)	JPL No.	Ave. No. of Twins/field	No. of S1 Carbide Particles	Ave. No. of Twins/mm	Grain boundary length/cm	Ave. No. of Disl./field	Ave. No. of Disl./ μm
19	5-685 A	24.40	37	347.085	1.22	2759.08	0.078
20	5-685 B	14.76	55	209.916	0.89	3702.18	0.105
21	5-685 C	21.25	21	302.189	1.39	2480.51	0.071
22	5-685 E	14.52	50	206.449	0.54	3595.42	0.102
23	5-685 F	20.76	27	295.247	1.08	2219.70	0.063
24	5-685 G	23.26	28	330.782	1.91	1191.12	0.034
25	5-685 H	19.10	48	271.659	0.88	1796.13	0.051
26	5-685 J	17.78	23	252.923	0.80	1818.59	0.052
27	5-685 K	12.87	30	182.978	1.82	2914.59	0.083
28	5-685 M	18.86	21	268.240	0.93	3536.89	0.101
29	5-685 N	15.45	28	219.769	1.15	2606.93	0.074
30	5-685 P	17.87	18	254.185	1.02	2960.46	0.084

TABLE 7

ANALYSIS OF MOBIL TYCO SAMPLES

MRI Sample # (Mobil Tyco)	JPL No.	Avg. No. of Twins/field	Avg. No. of Twins/mm ²	Grain boundary length/cm ²	Avg. No. of Dislocation Pits/field	Avg. No. of Dislocation Pits/μm ²
31	5-744 E	28.10	399.595	1.12	792.45	0.023
32	5-744 F	19.60	278.780	1.76	814.16	0.023
33	5-744 H	25.96	369.253	2.32	1161.55	0.033
34	5-744 G	22.05	313.650	2.51	1512.83	0.043
35	5-744 A	16.89	240.180	2.01	2704.46	0.077
36	5-744 B	29.35	417.464	1.20	1861.84	0.053
37	5-744 C	51.78	736.382	1.74	1189.71	0.034
38	5-744 D	59.35	844.084	0.74	1266.99	0.036

T A B L E 8

ANALYSIS OF MOBIL TYCO SAMPLES

MRI Sample No.	JPL No.	Avg. No. of Twins/field	Avg. No. of Twins/mm ²	Grain boundary length/cm ²	Avg. No. of Dislocation Pits/field	Avg. No. of Dislocation Pits/μm ²
39	5-742 A	38.83	552-220	1.76	2740.94	0.078
40	5-742 B	28.15	400.298	1.6	1798.02	0.051
41	5-742 C	53.75	764.416	1.50	949.78	0.027
42	5-742 D	46.79	665.410	1.57	846.78	0.024
43	5-742 E	45.57	648.059	0.80	1904.34	0.054
44	5-742 F	29.32	416.969	1.76	2705.71	0.077
45	5-742 G	49.34	701.677	2.11	1780.49	0.051
46	5-742 H	48.64	691.801	0.64	1979.37	0.056

TABLE 9

ANALYSIS OF MOBIL TYCO SAMPLES

MRI Sample #	JPL Sample #	No. of Twins/field	No. of Twins/mm ²	Grain boundary length/cm ²	No. of Dislocation Pits/field	No. of Dislocation Pits/μm ²
47	5-745 A	21.78	309.738	0.72	1949.83	0.055
48	5-745 B	53.10	755.151	1.93	1166.29	0.033
49	5-745 C	30.53	434.213	1.82	2428.95	0.069
50	5-745 D	60.51	860.580	3.44	1122.38	0.032
51	5-745 E	32.26	501.439	3.31	2583.40	0.073
52	5-745 F	43.63	620.473	2.30	1493.01	0.042
53	5-745 G	48.25	686.249	2.00	1556.36	0.044
54	5-745 H	59.19	841.787	1.84	1434.39	0.042

T A B L E 10

ANALYSIS OF MOBIL TYCO SAMPLES

MRI Sample #	JPL Sample #	No. of Twins/field	No. of Twins/mm ²	Grain boundary length/cm ²	No. of Dislocation Pits/field	No. of Dislocation Pits/ μm^2
55	5-743 A	55.18	784.721	2.27	1423.18	0.040
56	5-743 B	59.27	843.002	0.94	1465.18	0.042
57	5-743 C	40.06	569.736	1.96	1376.75	0.039
58	5-743 D	61.62	831.500	2.00	1189.66	0.034
59	5-743 E	56.23	799.764	2.04	1532.03	0.044
60	5-743 F	43.17	613.955	2.72	1885.17	0.054
61	5-743 G	59.86	851.352	2.48	1458.14	0.041
62	5-743 H	43.67	621.122	1.76	2190.90	0.062

TABLE 11

ANALYSIS OF MOBIL TYCO SAMPLES

MRI Sample #	JPL Sample #	No. of Twins/field	No. of Twins/mm ²	Grain boundary length/cm ²	No. of Dislocation Pits/field	No. of Dislocation Pits/μm ²
	(MRR #1)					
63	5-640 B	28.22	401.415	1.60	860.36	0.024
64	5-640 C	24.98	355.260	1.40	1136.35	0.032
65	5-640 D	24.57	349.427	2.52	1072.13	0.030
66	5-640 E	23.74	337.584	2.39	2427.54	0.069
67	5-640 F	48.55	690.422	2.19	860.34	0.025
68	5-640 G	18.67	265.506	1.08	1434.89	0.041
69	5-640 H	45.92	653.085	0.59	1245.87	0.035

T A B L E 12

ANALYSIS OF MOBIL TYCO SAMPLES

MRI Sample #	JPL Sample #	No. of Twins/field	No. of Twins/mm ²	Grain boundary length/cm ²	No. of Dislocation Pits/field	No. of Dislocation Pits/μm ²
	(MRR #2)					
70	5-640 A	20.21	287.431	1.92	976.88	0.028
71	5-640 B	39.75	565.332	2.76	576.89	0.016
72	5-640 C	24.08	342.460	2.60	685.26	0.019
73	5-640 D	22.14	314.947	2.19	850.34	0.024
74	5-640 E	50.11	712.701	2.00	621.43	0.018
75	5-640 F	30.21	429.695	1.55	842.55	0.024
76	5-640 G	42.22	600.411	1.82	998.84	0.028
77	5-640 H	35.90	510.569	2.35	650.94	0.019

T A B L E 13

ANALYSIS OF MOBIL TYCO SAMPLES

MRI Sample #	JPL Sample #	Twins/Field	Twins/mm ²	Grain Boundary Length	Dislocation Pits/field	Dislocation Pits/μm ²
78	5-867 A	32.7	834.18	4.85	1069.31	.0545
79	5-867 B	42.09	1073.76	0.76	494.86	.0252
80	5-867 C	27.91	712.02	2.78	994.35	.0507
81	5-867 D	50.58	1290.42	2.38	540.10	.0275
82	5-867 E	26.19	668.19	3.43	542.68	.0277
83	5-867 F	41.77	1065.63	2.06	373.79	.0191
84	5-867 G	24.27	619.21	3.37	635.78	.0324
85	5-867 H	36.65	934.94	2.07	440.21	.0224

Note: Samples 78-93 were examined by the Vidicon camera with a calibration factor of .00028 mm/pp and samples 94-105, and TYLAN #1 were examined by the Plumbicon camera using a calibration factor of .000366 mm/pp.

TABLE 14

ANALYSIS OF MOBIL TYCO SAMPLES

MRI Sample #	JPL Sample #	Twins/Field	Twins/mm ²	Grain Boundary Length	Dislocation Pits/field	Dislocation Pits/μm ²
86	5-867 I	-	-	-	-	-
87	5-867 J	21.29	543.18	4.71	1221.77	.0623
88	5-867 K	32.92	839.89	2.03	615.54	.0314
89	5-867 L	19.38	494.43	4.34	735.97	.0375
90	5-867 M	32.71	834.415	3.04	501.36	.0255
91	5-640 A	54.82	1398.61	2.76	362.87	.0185
92	5-640 B	22.81	581.86	3.68	537.89	.0274
93	5-640 C	50.02	1276.11	1.97	163.81	.0083
94	5-640 D	25.03	373.67	3.19	513.09	.0153

TABLE 15

ANALYSIS OF MOBIL TYCO SAMPLES

MRI Sample #	JPL Sample #	Twins/Field	Twins/mm ²	Grain Boundary Length	Dislocation Pits/Field	Dislocation Pits/μm ²
95	5-640 E	62.49	933.04	3.1	1182.93	.0340
96	5-640 F	28.92	446.3	5.15	999.09	.0298
97	5-640 G	51.70	771.92	3.4	641.73	.0192
98	5-640 H	23.39	360.98	4.38	886.58	.0264
99	5-990 A	36.02	537.85	2.54	867.54	.0259
100	5-990 B	30.39	453.74	3.52	1069.96	.0319
101	5-990 C	40.28	601.39	3.20	1396.13	.0417

T A B L E 16

ANALYSIS OF MOBIL TYCO AND HONEYWELL SAMPLES

MRI Sample #	JPL Sample #	Twins/Field	Twins/mm ²	Grain Boundary Length	Dislocation Pits/Field	Dislocation Pits/μm ²
102	5-990 E	37.96	566.76	1.52	1219.67	.0364
103	5-990 F	35.62	531.78	4.21	765.96	.0228
104	5-990 G	35.53	530.46	1.55	545.65	.0162
105	5-990 H	40.01	597.29	4.36	745.66	.0222
1 Honeywell	3-910	25.55	381.53	4.21	425.61	.0127

T A B L E 17

ANALYSIS OF MOBIL TYCO SAMPLES

MRI Sample #	JPL Sample #	Twins/Field	Twins/mm ²	Grain Boundary Length/cm ²	Dislocation Pits/Field	Dislocation Pits/μm ²
106	184-88 A	53.30	795.85	2.06	1245.8	.0372
107	184-88 B	45.72	682.58	2.11	794.08	.0237
108	184-88 C	42.76	638.38	2.00	496.78	.0148
109	184-88 D	47.06	702.67	1.82	1242.08	.0371
110	184-88 E	38.79	579.21	3.05	830.12	.0248
111	184-88 F	50.95	760.64	2.59	1175.68	.0351
112	184-88 G	38.66	577.21	2.99	1223.92	.0365
113	184-88 H	53.47	798.39	4.00	1206.46	.0360

T A B L E 18

ANALYSIS OF MOBIL TYCO SAMPLES

MRI Sample #	JPL Sample #	Twins/Field	Twins/mm ²	Grain Boundary Length/cm ²	Dislocation Pits/Field	Dislocation Pits/μm ²
114	184-175A	70.18	1047.83	2.91	672.33	.0200
115	184-175B	58.13	867.96	2.0	890.19	.0266
116	184-175D	53.97	805.84	2.09	1001.76	.0349
117	184-175E	53.46	798.25	1.57	1051.01	.0304
118	184-175F	54.79	818.05	2.03	1264.04	.0377
119	184-175H	57.00	851.09	3.05	681.88	.0204

T A B L E 19

ANALYSIS OF MOBIL TYCO SAMPLES

MRI Sample #	JPL Sample #	Twins/Field	Twins/mm ²	Grain Boundary Length/cm ²	Dislocation Pits/Field	Dislocation Pits/μm ²
120	5-1094-33A	18.99	283.63	4.06	1863.86	.0556
121	5-1094-33B	29.13	435.05	3.61	703.59	.0210
122	5-1094-33C	8.49	126.89	3.54	1637.14	.0488
123	5-1094-33D	16.47	245.88	2.64	814.78	.0243
124	5-1094-33E	19.66	293.49	3.31	1228.40	.0367
125	5-1094-33G	31.19	465.81	2.8	762.40	.0227
126	5-1094-33H	21.42	319.86	3.33	927.35	.0277

T A B L E 20

ANALYSIS OF MOBIL TYCO SAMPLES

MRI Sample #	JPL Sample #	Twins/Field	Twins/mm ²	Grain Boundary Length/cm ²	Dislocation Pits/Field	Dislocation Pits/μm ²
127	5-1092-69A	51.80	773.53	4.11	777.55	.0232
128	5-1092-69B	26.11	389.82	3.10	890.47	.0266
129	5-1092-69C	47.08	702.97	3.57	622.08	.0186
130	5-1092-69D	29.25	436.79	2.74	579.24	.0173
131	5-1092-69E	33.59	501.52	2.72	936.01	.0279
132	5-1092-69F	30.05	448.60	2.93	982.41	.0293
133	5-1092-69G	44.96	671.28	1.92	881.26	.0263
134	5-1092-69H	37.63	561.89	2.96	834.82	.0249

T A B L E 21

ANALYSIS OF IBM SAMPLES

MRI Sample No.	JPL No.	Avg. No. of Twins/field	Avg. No. of Twins/mm ²	Grain boundary length/cm ²	Avg. No. of Dislocation Pits/field	Avg. No. of Dislocation Pits/μm ²
1	4-457 A	43.70	621.581	1.3	460.56	0.013
2	4-457 B	41.30	587.374	1.5	205.37	0.006
3	4-457 C	39.96	568.254	1.12	373.20	0.011
4	4-457 D	37.25	529.826	0.51	302.98	0.009
5	4-457 E	29.82	424.114	0.52	328.91	0.010
6	4-457 F	38.09	541.730	1.33	405.75	0.012
7	4-457 G	15.79	224.585	1.5	342.75	0.010

TABLE 22

ANALYSIS OF MOTOROLA SAMPLES

MR I Sample #	JPL Sample #	No. of Twins/field	No. of Twins/mm ²	Grain boundary length/cm ²	No. of Dislocation Pits/field	No. of Dislocation Pits/ μ m ²
1	6-656 A	21.02	563.31 .	0.48	406.58	.0207 .
2	6-656 B	67.99	1734.66 .	0.7	196.17	.0100 .
3	6-656 C	21.59	550.77 .	2.12	310.58	.0158 .
4	6-656 D	73.01	1862.59 .	1.25	300.47	.0151 .
5	6-656 E	79.20	2020.60 .	2.05	195.65	.0099 .
6	6-656 F	32.16	820.39 .	3.12	155.85	.0079 .
7	6-656 G	50.59	1290.68 .	2.96	240.21	.0122 .
8	6-656 H	71.45	1822.78 .	3.07	305.25	.0155 .

TABLE 23
ANALYSIS OF MOTOROLA SAMPLES

MR I Sample #	JPL Sample #	No. of Twins/field	No. of Twins/ μm^2	Grain boundary length/ cm^2	No. of Dislocation Pits/field	No. of Dislocation Pits/ μm^2
9	6-656 I	63.12	1610.28	2.34	91.66	.0046
10	6-791 A	43.80	1117.41	0.54	388.44	.0198
11	6-791 B	71.90	1834.39	0.93	672.66	.0343
12	6-791 C	81.21	2071.94	1.43	352.01	.0179
13	6-791 D	70.98	1810.88	3.09	210.22	.0107
14	6-791 E	27.63	704.82	3.55	469.01	.0239
15	6-791 F	9.66	246.42	3.25	141.44	.0072
16	6-792 A	32.12	819.35	3.00	771.47	.0393

TABLE 24

ANALYSIS OF MOTOROLA SAMPLES

Mr I Sample #	JPL Sample #	No. of Twins/field	No. of Twins/ μm^2	Grain boundaries length/ μm^2	No. of Dislocation Pits/field	No. of Dislocation Pits/ μm^2
17	6-792 B	39.90	1017.91 .	3.705	408.21	.0208 .
18	6-792 V	25.88	660.28 .	3.33	429.62	.0219 .
19	6-792 D	33.85	863.63 .	4.08	225.91	.0115 .
20	6-792 E	37.74	962.73 .	3.50	108.75	.0055 .
21	6-792 F	21.87	557.97 .	5.48	103.36	.0052 .
22	6-840 A	31.46	802.77 .	5.74	256.57	.0129 .
23	6-840 B	16.88	430.62 .	6.93	131.89	.0067 .
24	6-840 C	16.35	417.11 .	4.93	136.07	.0069 .

TABLE 25

ANALYSIS OF MOTOROLA SAMPLES

MR I Sample #	JPL Sample #	No. of Twins/field	No. of Twins/mm ²	Grain boundary length/cm ²	No. of Dislocation Pits/field	No. of Dislocation Pits/ μ m ²
25	6-840 D	49.86	1272.02	4.20	28.12	.0014
26	6-840 E	22.85	582.97	2.95	101.41	.0052
27	6-840 F	35.95	917.21	4.87	77.46	.0039
28	6-840 G	6.18	157.91	5.88	51.15	.0026
29	6-837 A	27.15	692.71	2.16	486.63	.0248
30	6-837 B	48.13	1227.71	2.87	320.55	.0163
31	6-837 C	33.91	865.15	5.52	404.38	.0206
32	6-837 D	28.26	721.02	4.63	182.76	.0093

TABLE 26

```

5 REM*****PROGRAM-DEFECTS IN SILICON-VERSION 3(8/1/79)*****
6 REM*****ALL DATA IS OUTPUT FOR STORAGE ON FILE(DX1:)*
7 REM
8 DIM Z(1000)
9 PRINT "DEFECTS IN SILICON(VERSION 3-8/1/79)"
10 PRINT "HEADING"\PRINT
11 INPUT H$
15 PRINT "PRINT FILE NAME FOR STORAGE OF DATA(DX1:NAME)"
16 PRINT
17 INPUT A$
18 OPEN A$ FOR OUTPUT AS FILE #1
22 PRINT "OPERATOR"
23 PRINT
24 INPUT O$
30 PRINT "MAGNIFICATION"
31 PRINT
32 INPUT M$
40 PRINT "UNITS"
41 PRINT
42 INPUT U$
50 PRINT "CALIBRATION FACTOR(UNITS/PP)"
51 PRINT
52 INPUT C
60 PRINT "FRAME AREA(PP)"
61 PRINT
62 INPUT R
70 PRINT "QTM OUTPUT DATA DIVIDED BY"
71 PRINT
72 INPUT X
80 PRINT "AVERAGE FEATURE AREA(PP)"
81 PRINT
82 INPUT E
85 PRINT #1:"DEFECTS IN SILICON(VERSION 3-8/1/79)"\PRINT #1:
86 PRINT #1:H$\PRINT #1:
87 PRINT #1:"OPERATOR IS ";O$;" MAGNIFICATION=";M$
88 PRINT #1:"UNITS=";U$;" CALIBRATION FACTOR (UNITS/PP)=";C
89 PRINT #1:"FRAME AREA=";R;" QTM OUTPUT WAS DIVIDED BY";X;" AND CORRECTED"
90 PRINT #1:"AVERAGE FEATURE AREA (PP)=";E
91 PRINT #1:
95 PRINT #1:"FLD NO. NO./AREA MFPV MFPH L/A"
96 PRINT #1:"(A,P,VP,HP)"
100 PRINT "FLD NO. NO./AREA MFPV MFPH L/A"
101 PRINT "(A,P,VP,HP)"
106 REM
107 REM QTM MEASUREMENT ROUTINE
108 REM
109 CALL "CIFI"
110 CALL "STRT"(Z,4,"FIFI/CIF/FC1/FC2")
112 CALL "CIFW"("AC0,")
114 CALL "CIFW"("AE4,")
120 CALL "STEP"(1,"FIFI=FLD/FC1=A/FC2=A")
130 CALL "STEP"(2,"FC2=P")
140 CALL "STEP"(3,"FC2=VP")

```

ORIGINAL PAGE IS
OF POOR QUALITY

Table 26 (contd.)

```

150 CALL 'STEP'(4, 'FC2=HF')
160 INPUT B$
161 IF B$='D' THEN 610 \IF F=0 THEN 164
162 PRINT #1;F;N;G,M1,M2,L
163 PRINT #1;'(';A;P;V;H;')'
164 IF B$='A' THEN 700
165 IF B$='END' THEN 999
168 CALL 'SEQ'(1,2,3,4)
170 CALL 'FLD'(A,P,V,H)
180 CALL 'CIFM'('AU,')
190 F=F+1
200 A=X*A\P=F*X\V=V*X\H=H*X
209 REM
210 REM CALCULATION ROUTINE
211 REM
220 N=A/E
230 G=N/R/C/C
235 IF V=0 THEN 250
236 M1=R*KC/V
240 IF H=0 THEN 255
242 M2=R*C/H
243 GO TO 260
250 LET M1=0\GO TO 240
255 LET M2=0\GO TO 260
260 L=P/2/R/C
270 N1=N+N1\G1=G+G1\L1=L+L1
275 N2=N*N+N2\G2=G*G+G2\L2=L*L+L2
280 H1=H1+H\V1=V1+V
499 REM
500 REM PRINT OUT RESULTS
501 REM
530 PRINT F;N;G,M1,M2,L
531 PRINT '(';A;P;V;H;')'
550 GO TO 160
599 REM
600 REM DELETE LAST FIELD
601 REM
610 N1=N1-N\N2=N2-N*N
615 G1=G1-G\G2=G2-G*G
620 L1=L1-L\L2=L2-L*L
625 F=F-1\H1=H1-H\V1=V1-V
630 PRINT 'LAST FIELD DELETED'
635 INPUT B$
640 GO TO 164
699 REM
700 REM *****AVERAGE,SD,SE*****
701 REM
710 LET Z1=N1/F
720 LET Z2=G1/F
730 IF V1=0 THEN 750
735 LET Z3=F*R*KC/V1
740 IF H1=0 THEN 755
745 Z4=F*R*C/H1
746 GO TO 760
750 LET Z3=0\GO TO 740
755 LET Z4=0
760 LET Z5=L1/F
770 LET D=N2/F-Z1*Z1
780 LET S1=SQR(D)

```

Table 26 (contd.)

```

781 LET E1=S1/(SQR(F))
790 LET D=G2/F-Z2*Z2\IF D<0 THEN 801
800 LET S2=SQR(D)\E2=S2/(SQR(F))\GO TO 810
801 LET S2=0\E2=0
810 LET D=L2/F-Z5*Z5
811 IF D<0 THEN 821
820 LET S5=SQR(D)\E5=S5/(SQR(F))\GO TO 850
821 LET S5=0\E5=0
850 PRINT '
851 PRINT '          NO.          NO./AREA          MFPV          MFPH          L/A'
852 PRINT #1:'          *****AVERAGE*****'
853 PRINT #1:'          NO.          NO./AREA          MFPV          MFPH          L/A'
860 PRINT '      ;Z1,Z2,Z3,Z4,Z5
861 PRINT #1:'      ;Z1,Z2,Z3,Z4,Z5
870 PRINT 'SD';S1,S2,,,S5
871 PRINT #1:'SD';S1,S2,,,S5
880 PRINT 'SE';E1,E2,,,E5
881 PRINT #1:'SE';E1,E2,,,E5
898 INPUT B#
900 GO TO 164
999 END
*
```

TABLE 27. - QTM Data of Wacker Sample #7
TEST RUN 10/11/78 WACKER SAMPLE #7
TWINS ONLY

MAG-111.3 UNITS-MM CAL. FACTOR- 1.788964 UNITS/PP
 FRAME AREA- 3.464648

FIELD NO.	NO./AREA	MFPV	MFPH	L/A	AFETA	
1	10	21.522	8.217	8.143	9.294	1.183712
2	8	17.217	1.315	1.156	7.917	1.182949
3	6	12.913	1.154	1.144	7.216	1.182275
4	14	38.138	3.147	1.154	10.297	1.181814
5	7	13.865	1.267	1.261	5.194	1.181778
6	5	13.761	8.527	1.264	4.626	1.181727
7	1	2.152	8.833	4.869	1.268	1.181627
8	5	13.761	1.187	1.444	1.142	1.181127
9	8	17.217	8.147	1.578	7.476	1.182079
10	15	32.283	3.185	1.257	7.147	1.181941
AVERAGE						
	NO.	NO./AREA	MFPV	MFPH	L/A	AFETA
SD	7.97	17.132	1.157	1.767	4.245	1.182415
SE	4.31	8.633	2.139	1.176	2.499	1.181111
	1.27	2.738	1.737	1.405	1.927	1.181711
11	17	21.522	1.296	8.214	7.129	1.182877
12	17	21.522	8.272	1.234	5.227	8.181869
13	1	2.152	4.335	1.274	1.474	1.181711
14	9	19.378	8.448	1.186	4.177	1.182777
15	3	6.457	1.467	1.219	1.418	1.181467
16	6	12.913	1.311	1.268	1.492	1.181727
17	8	17.217	1.183	1.112	1.278	1.181527
18	11	23.674	8.157	1.258	2.224	1.181199
19	3	6.457	8.692	1.147	1.499	1.181491
20	7	15.765	1.296	1.267	4.481	1.182625
AVERAGE						
	NO.	NO./AREA	MFPV	MFPH	L/A	AFETA
SD	7.35	15.218	1.976	1.767	5.716	1.182547
SE	3.71	7.974	1.275	1.172	1.167	1.181425
	3.03	1.783	1.119	1.262	1.788	1.181711
21	2	1.774	2.452	1.497	1.487	1.181867
22	7	15.765	1.186	1.137	4.228	1.181199
23	8	17.217	1.248	1.147	8.297	1.181457
24	6	12.917	1.477	1.277	4.172	1.181557
25	4	8.439	1.841	1.327	1.446	1.181777
26	8	17.217	1.287	1.115	1.135	1.181777
27	4	8.439	1.346	1.575	1.877	1.181987
28	4	8.439	1.413	1.261	4.817	1.181777
29	5	13.761	5.671	1.221	1.472	1.181747
30	9	19.378	1.172	1.499	1.578	1.181178
31	5	13.761	1.158	1.128	1.177	1.181288
32	4	8.639	1.149	1.568	1.121	1.181747
AVERAGE						
	NO.	NO./AREA	MFPV	MFPH	L/A	AFETA
SD	6.66	14.125	1.162	1.485	5.171	1.182061
SE	3.13	7.113	1.758	1.269	1.948	1.181924
	8.58	1.257	8.111	1.171	1.521	1.181747
33	8	17.217	8.155	1.275	4.734	1.182415
34	4	8.639	1.931	1.275	1.257	1.181617
35	5	13.761	1.298	1.188	1.227	1.181419
36	8	17.217	1.477	1.188	1.217	1.181451
37	3	6.457	8.623	1.116	1.915	1.181777
38	9	19.377	1.154	1.187	4.171	1.181377
39	13	21.522	1.168	1.177	11.271	1.181767
40	5	13.761	8.197	1.184	1.144	1.181117
41	9	19.378	8.175	1.194	4.540	1.181717
42	5	13.761	1.128	1.272	1.444	1.181727
43	12	25.326	1.477	1.491	1.187	1.181679
44	9	19.378	8.176	1.142	1.255	1.181719
45	19	48.891	1.171	1.168	12.417	1.181787
46	9	19.378	8.579	1.175	1.159	1.181577
47	18	38.779	1.148	1.142	11.497	1.181528
48	8	17.217	1.424	1.187	4.717	1.182526
49	7	15.865	1.444	1.494	1.177	1.181199
50	8	17.217	1.145	1.184	11.517	1.182151
AVERAGE						
	NO.	NO./AREA	MFPV	MFPH	L/A	AFETA
SD	7.18	15.283	1.862	1.577	5.147	1.182054
SE	3.75	8.163	1.447	1.271	1.147	1.181652
	3.73	1.148	1.234	1.117	1.487	1.181262

ORIGINAL PAGE IS
 OF POOR QUALITY

TABLE 28

MRI 100 JPL 5-990 SPEC B MOBIL TYCO AREA.78, TWINS ONLY

OPERATOR IS TIM MAGNIFICATION=800
 UNITS= MM CALIBRATION FACTOR (UNITS/PP)= 3.65000E-04
 FRAME AREA= 500000 RTM OUTPUT WAS DIVIDED BY 100 AND CORRECTED
 AVERAGE FEATURE AREA (PP)= 2601

FLD	NO.	NO./AREA	MFPV	MFPH	L/A
(A,P,VP,HP)					
1	56.1707	838.644	.114375	.0135556	77.5956
(146100	28400 1600	13500)		
2	46.4437	693.417	.107647	.0133577	78.6885
(120800	28800 1700	13700)		
3	6.42061	95.8614	.366	.038125	27.3224
(16700	10000 500	4800)		
4	4.65206	69.4565	.4575	.0590323	17.7596
(12100	6500 400	3100)		
5	0 0	0	0	0	
(0 0 0 0)				
6	0 0	0	0	0	
(0 0 0 0)				
7	0 0	0	0	0	
(0 0 0 0)				
8	0 0	0	0	0	

Table 28 (contd.)

(0 0 0 0)					
9 0 0 0	0	0	0		
(0 0 0 0)					
10 0 0 0	0	0	0		
(0 0 0 0)					
11 1.11496 16.6466	.61	.261429	4.37158		
(2900 1600 300 700)					
12 0 0 0	0	0	0		
(0 0 0 0)					
13 0 0 0	0	0	0		
(0 0 0 0)					
14 0 0 0	0	0	0		
(0 0 0 0)					
15 0 0 0	0	0	0		
(0 0 0 0)					
16 0 0 0	0	0	0		
(0 0 0 0)					
17 0 0 0	0	0	0		
(0 0 0 0)					
18 18.2238 272.086	.0732	.0237662	48.3607		
(47400 17700 2500 7700)					
19 32.2184 481.029	.0795652	.018866	59.0164		
(83800 21600 2300 9700)					
20 22.7605 339.82	.0871429	.01464	73.4973		
(59200 26900 2100 12500)					
21 49.8654 744.505	.0653571	9.89189E-03	106.831		
(129700 39100 2800 18500)					
22 23.7216 354.171	.101667	.0157759	68.0328		
(61700 24900 1800 11600)					
23 30.9112 461.513	.0963158	.0179412	59.8361		
(80400 21900 1900 10200)					
24 60.5921 904.656	.130714	.0147581	71.0383		
(157600 26000 1400 12400)					
25 117.724 1757.65	.0508333	7.06564E-03	150		
(306200 54900 3600 25900)					
*****AVERAGE*****					
	NO.	NO./AREA	MFPV	MFPH	L/A
	18.8328	281.178	.199782	.0317048	33.694
SD	28.2367	421.581			41.619
SE	5.64733	84.3162			8.32379
26 42.6759 637.163	.0915	8.75598E-03	118.033		
(111000 43200 2000 20900)					
27 90.3499 1348.95	.061	7.75424E-03	134.699		
(235000 49300 3000 23600)					
28 56.2476 839.792	.0795652	9.63158E-03	108.743		
(146300 39800 2300 19000)					
29 95.0788 1419.55	.0831818	.0132609	81.9672		
(247300 30000 2200 13800)					
30 75.2403 1123.36	.107647	.0240789	45.9016		
(195700 16800 1700 7600)					
31 79.5463 1187.65	.0703846	.0145238	73.224		
(206900 26800 2600 12600)					
32 69.3195 1034.96	.122	.015124	69.6721		
(180300 25500 1500 12100)					
33 90.7343 1354.69	.122	.0132609	79.235		
(236000 29000 1500 13800)					
34 51.7109 772.058	.166364	.0220482	48.3607		
(134500 17700 1100 8300)					

Table 28 (contd.)

35	93.1949	1391.43	.0677778	.012449	86.8853
(242400	31800	2700	14700)
36	29.6809	443.144	.183	.0494595	23.224
(77200	8500	1000	3700)
37	63.8216	952.874	.107647	.018866	57.377
(166000	21000	1700	9700)
38	84.5829	1262.85	.0915	.0207955	53.5519
(220000	19600	2000	8800)
39	22.1069	330.062	.0315517	.0205618	68.8525
(57500	25200	5800	8900)
40	5.22876	78.0668	.101667	.0677778	21.0383
(13600	7700	1800	2700)
41	4.95963	74.0487	.22875	.061	18.306
(12900	6700	800	3000)
42	.307574	4.59216	1.83	1.83	1.0929
(800	400	100	100)
43	.307574	4.59216	0	1.83	.819672
(800	300	0	100)
44	.192234	2.8701	0	1.83	.819672
(500	300	0	100)
45	1.1534	17.2206	.61	.366	3.82514
(3000	1400	300	500)
46	.692042	10.3324	.915	.305	3.82514
(1800	1400	200	600)
47	0	0	0	0	
(0	0	0	0)
48	24.6444	367.947	.22875	.0366	29.235
(64100	10700	800	5000)
49	45.2903	676.196	.1525	.0240789	44.5355
(117800	16300	1200	7600)
50	21.6455	323.174	.261429	.0290476	36.0656
(56300	13200	700	6300)

*****AVERAGE*****

NO.	NO./AREA	MFPV	MFPH	L/A
30.3906	453.74	.152755	.0263082	41.0328
SD 33.7557	503.982			40.7425
SE 4.77377	71.2738			3.76186

*TT:=DX1:MT100D.DAT

DEFECTS IN SILICON(VERSION 3-8/1/79)

MRI 100 JPL 5-990 SPEC B AREA .98, MOBIL TYCO DISLOCATIONS ONLY

OPERATOR IS TIM MAGNIFICATION=800

UNITS= MICRONS CALIBRATION FACTOR (UNITS/PP)= .366

FRAME AREA= 250000 QTM OUTPUT WAS DIVIDED BY 1 AND CORRECTED

AVERAGE FEATURE AREA (PP)= 10.6

FLD	NO.	NO./AREA	MFPV	MFPH	L/A
(A,P,VP,HP)					
1	270.566	8.07925E-03	110.909	90.2367	.0170929
(2868	3128	825	1014)
2	56.9811	1.70149E-03	455.224	448.529	3.66667E-03
(604	671	201	204)
3	113.585	3.39171E-03	224.816	227.047	7.43716E-03
(1204	1361	407	403)
4	237.83	7.10174E-03	129.42	119.921	.0134153
(2521	2455	707	763)
5	1950.75	.0582506	18.3957	17.6641	.0906776

C-2

Table 28 (contd.)

(20678 16594 4974 5180)					
6 288.491 8.61449E-03	96.6209	100.549	.0170273		
(3058 3116 917 910)					
7 1327.17 .03963	24.7632	26.2403	.064153		
(14068 11740 3695 3487)					
8 2299.91 .0686765	17.3526	16.6849	.0948689		
(24379 17361 5273 3484)					
9 3757.64 .112205	10.6062	11.3467	.148087		
(39831 27100 8627 8064)					
10 2434.81 .0727048	12.7811	13.3792	.126454		
(25809 23141 7159 6839)					
11 3774.53 .11271	11.6531	11.8877	.140109		
(40010 25640 7852 7697)					
12 613.679 .0183248	44.4823	47.0679	.0369071		
(6505 6754 2057 1944)					
13 1610.66 .0480952	18.7462	20.172	.0854918		
(17073 15645 4881 4536)					
14 817.925 .0244237	42.4397	39.4227	.040235		
(8670 7363 2156 2321)					
15 1554.25 .0464106	24.8169	23.5946	.0670219		
(16475 12265 3687 3878)					
16 619.057 .0184854	52.556	51.4334	.031306		
(6562 5729 1741 1779)					
17 611.415 .0182572	64.2017	59.648	.0262514		
(6481 4804 1412 1534)					
18 181.415 5.41715E-03	175.287	153.266	.010541		
(1923 1929 522 597)					
19 815.755 .0243589	42.4004	37.577	.0417049		
(8647 7632 2158 2435)					
20 306.887 9.16381E-03	116.561	101.554	.0161093		
(3253 2948 785 901)					
21 77.0755 2.30152E-03	363.095	371.951	4.65027E-03		
(817 851 252 246)					
22 19.9057 5.94394E-04	18300	1158.23	8.96175E-04		
(211 164 5 79)					
23 37.3585 1.11555E-03	756.198	491.935	2.40437E-03		
(396 440 121 186)					
24 38.1132 1.13808E-03	839.45	839.45	2.08197E-03		
(404 381 109 109)					
25 88.3962 2.63956E-03	307.047	312.287	5.35519E-03		
(937 980 298 293)					
*****AVERAGE*****					
NO.	NO./AREA	MFPV	MFPH	L/A	
956.166	.0285516	37.5918	37.5721	.0437578	
SD 1098.12	.0327904			.0449326	
SE 219.623	6.55808E-03			8.98652E-03	
26 245.566 7.33274E-03	129.972	121.353	.0132077		
(2603 2417 704 754)					
27 206.038 6.15240E-03	139.908	139.482	.0120109		
(2184 2198 654 656)					
28 8.11321 2.42265E-04	1386.36	1663.64	1.40437E-03		
(86 257 66 55)					
29 46.4151 1.38598E-03	915	610	2.34426E-03		
(492 429 100 150)					
30 4.33962 1.29584E-04	10166.7	2691.18	4.04372E-04		
(46 74 9 34)					
31 37.5472 1.12118E-03	809.735	795.652	2.02186E-03		
(398 370 113 115)					

Table 28 (contd.)

32	1,13208	3.38044E-05	45750	13071.4	1.58470E-04
(12 29 2 7)					
33	689,245	.0205812	48,2341	54,2062	.0317978
(7306 5819 1897 1688)					
34	506,792	.0151331	60,6362	60,1578	.0288852
(5372 5286 1509 1521)					
35	344,528	.0102878	78,8793	82,6558	.0211038
(3652 3862 1160 1107)					
36	5095,19	.152145	15,154	14,8106	.109721
(54009 20079 6038 6178)					
37	5326,98	.159067	13,6853	12,3548	.127393
(56466 23313 6686 7406)					
38	980,566	.0292802	31,1225	28,5759	.0564262
(10394 10326 2940 3202)					
39	2612,45	.0780093	14,2612	13,1787	.11776
(27692 21550 6416 6943)					
40	2614,91	.0780825	17,2968	16,1205	.0937596
(27718 17158 5290 5676)					
41	2856,51	.085297	16,5551	15,8799	.102432
(30279 18745 5527 5762)					
42	3101,23	.0926043	13,5135	13,3382	.122038
(32873 22333 6771 6860)					
43	2443,87	.0729752	17,6335	15,3652	.100011
(25905 18302 5189 5955)					
44	1198,77	.035796	27,8624	27,071	.0586776
(12707 10738 3284 3380)					
45	607,453	.0181389	61,908	59,6869	.0275956
(6439 5050 1478 1533)					
46	25,9434	7.74684E-04	1039,77	682,836	1.86339E-03
(275 341 88 134)					
47	58,1132	1.73529E-03	933,673	1433,93	7.97814E-04
(616 146 98 56)					
48	.849057	2.53533E-05	18300	7625	4.64481E-04
(9 85 5 12)					
49	0 0 0	0	0	0	
(0 0 0 0)					
50	581,415	.0173614	75,5574	64,5275	.0238251
(6163 4360 1211 1418)					

*****AVERAGE*****

	NO.	NO./AREA	MFPV	MFPH	L/A
	1069.96	.0319497	38.743	37.659	.043001
SD	1353.36	.040412			.0453395
SE	191.393	5.71512E-03			6.41197E-03

*TT:=DX1:MT101T.DAT

DEFECTS IN SILICON(VERSION 3-8/1/79)

MRI 101 JPL 5-990 SPEC C MOBIL TYCO AREA ,98 TWINS ONLY

OPERATOR IS TIM MAGNIFICATION=800

UNITS= MM CALIBRATION FACTOR (UNITS/PP)= 3.66000E-04

FRAME AREA= 500000 RTM OUTPUT WAS DIVIDED BY 100 AND CORRECTED

AVERAGE FEATURE AREA (FF)= 2453

FLD	NO.	NO./AREA	MFPV	MFPH	L/A
(A,F,VP,HP)					
1	18,7525	279,981	.0703846	.0244	49,7268
(46000 18200 2600 7500)					
2	56,8284	848,463	.0631034	9,89189E-03	108,197